Quantum and classical random walks

A comprehensive introduction to QRW simulations

Tristan Dobrian

Physics Department, University of Colorado at Boulder

Abstract

This is a comprehensive and self-contained introduction to the math that underlies classical random walks and quantum random walk simulations.

Introduction

A random walk simulates the random movement of a particle through space. A classical random walk simulates the random movement of a point-like particle (or a particle's center of mass) through space, while a quantum random walk simulates the movement of a de Broglie wave through space. These two kinds of random walks have very different probability distributions of the particle's position in space, with the distributions differing in both, their appearance and in their statistical properties.

Probably the most significant qualitative difference between classical and quantum random walks, is that the probability mass for a classical particle tends to center around the particle's initial position, while the probability mass of a quantum particle tends to spread out, away from the particle's initial position [1]. A classical particle is most likely to be found at its initial position, while a quantum particle is generally least likely to be found at its initial position.

The difference in statistical properties between classical and quantum random walks is another important difference [1–5]. The probability distribution after the n^{th} step of a classical random walk on a line takes on a binomial distribution, and thus has a variance of $\sigma^2 \sim n$, so that the we can expect to find the particle a distance $O(\sqrt{n})$ from its initial position. In contrast, the variance of a Hadamard quantum random walk on a line grows as $\sigma^2 \sim n^2$, so we can expect to find a quantum particle a distance $O(n)$ from its initial position [2]. This means that the particle in a Hadamard quantum random walk on a line tends to spread out quadratically faster than does the particle in a classical random walk on a line. The unusual appearance of a quantum random walk distribution can be attributed to the wavelike interference that is characteristic of quantum particles.

How this paper is structured

Part 1 introduces basic examples of classical random walks, beginning with a discrete random walk on a line and a computation of its statistical properties. We then show that the gamma function can be used to create a continuous curve that traces out the probability mass points of the discrete distribution. This is followed by a formal approach to taking the continuous limit of a discrete classical random walk on a line, and a discussion on how it compares to the gamma-function-continuous version. The part on classical random walks concludes with classical random walks in higher dimensions, which take on multinomial distributions.

Part 2 begins by introducing a quantum random walk on a line, using the Hadamard coin operator, along with a calculation of the quantum walk's statistical properties. We then show how modifying the initial state and coin operator can be used to give a distribution that is symmetric about $x = 0$. This is followed by a Hadamard walk in the presence of an absorbing boundary, and a comparison of its predictions with what would be predicted classically. This is followed with a quantum walk on a circle, a discussion of conservation of information during a quantum walk, and how the coin operator of a quantum walk can be

modified to a nonunitary version that gives rise to a distribution that very closely resemble the distribution that is seen for a classical random walk on a line.

We then consider two different generalizations of the Hadamard walk on a line, to a Hadamard walk in two spatial dimensions, using both the $H^{\otimes 2}$ and DFT_2 coin operators. This is followed by a Hadamard walk on a topological torus. We then give an example of a weird prediction that quantum mechanics makes for quantum random walks, which is then followed by a derivation of the Klein-Gordon equation, starting from a quantum random walk.

1 Part 1: Classical random walks

The aim in modeling a process as a random walk is to determine the probability distribution of the particle's position in space after a specified number of time steps. This amounts to finding a probability mass function $Prob(x = i)$ that tells us the probability that the particle will land at position $x = i$ at the end of its N^{th} step.

1.1 Classical Random Walk on a Line

The work done in this section draws primarily from [6–8]. Consider a classical particle initially located at $x = 0$ of the real line. This axis can be discretized by defining $x = il$ for a fixed constant l, and then labeling points accessible to the particle by integer values of i. For simplicity let us choose to work in units where $l = 1$. Similarly, we can partition the time evolution of the particle's motion into N discrete time steps, by defining $t = N\tau$ and then taking τ into our units so that $t = N$. Let $N = 0$ at the start of the particle's random walk.

Each time step is initiated by a coin flip. If the coin lands heads the particle moves right, from position $x = i$ to $i + 1$. If the coin lands tails, the particle moves left, from i to $i - 1$. The particle never stays at the same position during a time step, it has to move either right or left. We can allow the coin to have a biased tendency toward landing heads or tails by introducing a constant p_r to represent the probability that the particle moves right, and $p_l = 1 - p_r$ to represent the probability that the particle steps left.

After the particle's N^{th} step, it has taken n_r steps to the right and n_l steps to the left, which gives us the useful condition $n_r + n_l = N$. This will allows us to eliminate n_l in favor of n_r and N.

Our objective is to find a function $Prob\,(i, N)$ that gives the probability for the particle to land at position $x = i$ at the end of its N^{th} step. Since each step is an independent event, each rightward or leftward step contributes a multiplicative factor of p_r or $p_l = 1 - p_r$ to the total probability for the particle to land at $x = i$ on its N^{th} step. So the probability that the particle will take n_r steps to the right, and $n_l = N - n_r$ steps to the left is ${p_r}^{n_r}{p_l}^{n_l}$, or

$$ {p_r}^{n_r}\,(1 - p_r)^{N - n_r} \tag{1} $$

The particle will always end up at the same position $x = i$ when it takes a total of n_r steps to the right and n_l steps to the left, regardless of the order the steps are taken in. Each path that has exactly n_r steps to the right and n_l steps to the left contributes one factor of ${p_r}^{n_r} (1 - p_r)^{N-n_r}$ to the total probability for the particle to land at $x = i$ on its N^{th} step. If the particle takes N total steps, then there are $\binom{N}{n_r}$ ways to choose n_r of these steps to be rightward. Each permutation corresponds to its own distinct path, so there are $\binom{N}{n_r}$ N-step paths that the particle can take to end up at $x = i$ on its N^{th} step. Since each path is equally likely, the total probability that the particle will land at $x = i$ on its N^{th} step is

$$Prob\,(R = n_r) = f(n_r) = \binom{N}{n_r} {p_r}^{n_r} (1 - p_r)^{N-n_r} \tag{2}$$

where R is a binomial random variable that keeps track of the total number of rightward steps. I've defined the probability mass function $f(n_r)$ because it is convenient for plotting the probability distribution of the particle's position using computer software.

It is generally more useful to have a function that represents the probability for the particle to land at position $x = i$ than it is to have a function that takes n_r as its parameter. We can make that happen by rewriting (2) as a function of the particle's final position $x = i$, instead of as a function of the particle's number of rightward steps $R = n_r$.

We can turn (2) into the probability that the particle lands at $x = i$ on its N^{th} step by finding a parameterization $n_r = n_r\,(x)$, and substituting it into (2) in place of n_r.

To find an expression $n_r = n_r(x)$, note that the particle lands at position $i = n_r - n_l = 2n_r - N$ on its N^{th} step, which rearranges to,

$$n_r = \tfrac{1}{2}(i + N) \tag{3}$$

Substituting this into (2), the probability that the particle will be at position $x = i$ after its N^{th} step is

$$Prob\,(x = i) = \begin{cases} 0 & \text{if } \frac{1}{2}\,(i + N) \mod 1 \neq 0 \\ f\left(\frac{1}{2}\,(i + N)\right) & \text{otherwise} \end{cases} \tag{4}$$

where $Prob(x = i) = 0$ if $\frac{1}{2}\,(i + N) \mod 1 \neq 0$ is a required condition when plotting the probability distribution as a function $Prob\colon \mathbb{Z} \to \mathbb{R}$, $i \mapsto f\left(\frac{1}{2}\,(i + N)\right)$ or else you'll get nonzero probability for half-integer steps.

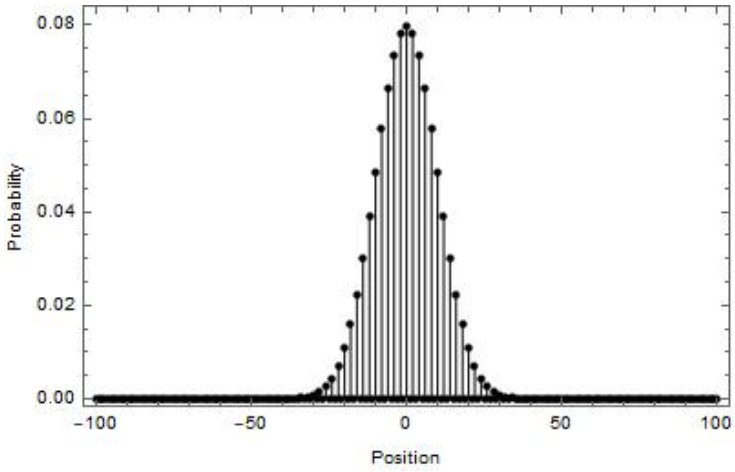

Figure 1: The probability distribution after $N = 100$ steps of a classical random walk on a line. This distribution was plotted for probability of rightward step $p_r = \frac{1}{2}$. The probability mass points of zero mass occur all along the x-axis, at odd values of x, because the particle always lands on even/odd values of x for even/odd values of N. So the fact that $N = 100$ is even, means that there is zero probability for the particle to land on an odd value of x.

The probability distribution of the particle's position after taking $N = 100$ steps in an unbiased classical random walk is shown in Figure 1. It will be shown in the upcoming subsection that the mean and variance of an N-step classical random walk are $\langle x \rangle = N(p_r - p_l)$ and $\sigma^2 = 4Np_rp_l$. So the random walk shown in Figure 1 has a mean position $\langle x \rangle = 0$ and expected distance from the origin $\sigma = 10$.

As a consistency check, it can be quickly shown using computational software that

$$\sum_{i=-100}^{100} Prob\,(x = i, N = 100) = 1$$

where I've written the probability mass function as an explicit function of N to make it clear that the particle took a total of 100 steps.

1.2 Expectation and Variance

The expectation value for the particle's position after N steps is given by,

$$\langle x \rangle = \sum_{i=-N}^{N} i \cdot Prob\,(x = i) \tag{5}$$

where points outside of $[-N, N]$ have been excluded from the summation, since $Prob\,(|x| > N) = 0$. A second, shorter approach to deriving $\langle x \rangle$ in the appendix A.1, which uses the fact that the laws of physics are invariant under spatial translation to bypass pretty much all of the rigor that is shown in this section.

Using $x = n_r - n_l$ and linearity of the expectation value,

$$\begin{aligned}\langle x\rangle &= \langle n_r\rangle - \langle n_l\rangle \\ &= \sum_{i=0}^{N} i\cdot Prob\left(n_r = i\right) - \sum_{j=0}^{N} j\cdot Prob\left(n_l = j\right) \\ &= \sum_{i=1}^{N} i\cdot \binom{N}{i} {p_r}^i \left(1-p_r\right)^{N-i} - \sum_{j=1}^{N} j\cdot \binom{N}{j} {p_l}^j \left(1-p_l\right)^{N-j} \end{aligned} \tag{6}$$

where the last line comes from substitution of (2) into the second line of (6) and incrementing the index's starting value from 0 to 1 on both summations, since the first term in each summation is equal to zero. An important point is that each summation in (6) is over $i, j \in [0, N]$, as opposed to the summation over $i \in [-N, N]$ that appears in (5). This happens because the quantities n_r, n_l represent the number of steps in one direction, either right or left, along the x-axis, while x takes into account the total number of steps in both directions.

Taking the first summation from (6) and pulling a factor of N out of $\binom{N}{i} = \frac{N!}{i!(N-i)!}$

$$\begin{aligned}\sum_{i=1}^{N} i\cdot \binom{N}{i} {p_r}^i \left(1-p_r\right)^{N-i} &= \sum_{i=1}^{N} i\cdot \frac{N\left(N-1\right)!}{i!\left(N-i\right)!} {p_r}^i \left(1-p_r\right)^{N-i} \\ &= Np_r \sum_{i=1}^{N-1} \frac{\left(N-1\right)!}{\left(i-1\right)!\left[\left(N-1\right)-\left(i-1\right)\right]!} {p_r}^{i-1} \left(1-p_r\right)^{N-i} \\ &= Np_r \sum_{i=1}^{N-1} \binom{N-1}{i-1} {p_r}^{i-1} \left(1-p_r\right)^{N-i} \end{aligned} \tag{7}$$

Substituting $M = N-1$ and $k = i-1$ into the summation on the right hand side of (7) and using the binomial theorem[1]

$$\begin{aligned}\sum_{i=1}^{N} i\cdot \binom{N}{i} {p_r}^i \left(1-p_r\right)^{N-i} &= Np_r \sum_{k=0}^{M} \binom{M}{k} {p_r}^k \left(1-p_r\right)^{M-k} \\ &= Np_r \left[p_r + \left(1-p_r\right)\right]^M \\ &= Np_r \end{aligned} \tag{8}$$

Applying substituting this into (6), applying the same procedure to the second term in (6) gives,

$$\langle x\rangle = N\left(p_r - p_l\right) \tag{9}$$

As a quick consistency check, it's worth noting that (9) equals $-N, 0, N$, for the three special cases of $p_r = 0, \frac{1}{2}, 1$, which is what we should expect.

[1]The binomial theorem: $\left(x+y\right)^n = \sum_{i=0}^{n} \binom{n}{i} x^i y^{n-i}$

1.3 The variance

Finding the variance $\sigma^2 = \langle x^2 \rangle - \langle x \rangle^2$ requires that we first find $\langle x^2 \rangle$.

$$\begin{aligned} \left\langle x^2 \right\rangle &= \left\langle (n_r - n_l)^2 \right\rangle \\ &= \left\langle (2n_r - N)^2 \right\rangle \\ &= 4 \left\langle {n_r}^2 \right\rangle + N^2 - 4N \langle n_r \rangle \end{aligned} \tag{10}$$

where

$$\left\langle {n_r}^2 \right\rangle = \sum_{i=0}^{N} i^2 \cdot Prob\left(n_r = i\right) \tag{11}$$

Inserting (2) into (11) and carrying out the exact same steps as was done in (7), with the extra factor of i left out of the equation modifications gives

$$\left\langle {n_r}^2 \right\rangle = N p_r \sum_{i=1}^{N-1} i \cdot \binom{N-1}{i-1} {p_r}^{i-1} \left(1 - p_r\right)^{N-i} \tag{12}$$

Using $M = N - 1, j = i - 1$ into (12) gives,

$$\begin{aligned} \left\langle {n_r}^2 \right\rangle &= N p_r \sum_{j=0}^{M} (j+1) \cdot \binom{M}{j} {p_r}^{j} \left(1 - p_r\right)^{M-j} \\ &= N p_r \sum_{j=0}^{M} (j+1) \cdot \binom{M}{j} {p_r}^{j} \left(1 - p_r\right)^{M-j} \\ &= N p_r \sum_{j=0}^{M} j \cdot \binom{M}{j} {p_r}^{j} \left(1 - p_r\right)^{M-j} + N p_r \sum_{j=0}^{M} \binom{M}{j} {p_r}^{j} \left(1 - p_r\right)^{M-j} \end{aligned} \tag{13}$$

The second summation on the right hand side $\sum_{j=0}^{M} \binom{M}{j} {p_r}^{j} \left(1 - p_r\right)^{M-j} = 1$, since the sum over all probabilities is always equal to one. So the second term is equal to $N p_r$. Comparing the summation in the first term on the right hand side of (13) with (8), it's easy to see that it has the same form as the expectation value of a binomial random variable with parameters (M, p_r). Since $M = N - 1$, the summation in the first term is equal to $(N-1)\, p_r$, so

$$\left\langle {n_r}^2 \right\rangle = N p_r \left[(N-1)\, p_r + 1\right] \tag{14}$$

Substituting (14) into (10), and then grouping terms by powers of N

$$\begin{aligned} \left\langle x^2 \right\rangle &= 4 \left(N^2 {p_r}^2 - N {p_r}^2 + N p_r\right) + N^2 - 4N \langle n_r \rangle \\ &= \left(4 {p_r}^2 - 4 p_r + 1\right) N^2 + 4 p_r \left(1 - p_r\right) N \end{aligned} \tag{15}$$

Using $\langle n_r \rangle = Np_r$ to replace terms in (15) that are proportional to N^2, substituting $p_l = 1 - p_r$ into the term that is proportional to N, and then using linearity of the expectation value

$$\begin{aligned}
\left\langle x^2 \right\rangle &= \left(\left(2 \langle n_r \rangle\right)^2 - 2\left(2p_r\right) + N \right) + 4Np_r p_l \\
&= \left(2 \langle n_r \rangle - N\right)^2 + 4Np_r p_l \\
&= \langle 2n_r - N \rangle^2 + 4Np_r p_l \\
&= \langle x \rangle^2 + 4Np_r p_l
\end{aligned} \tag{16}$$

with the transition between the third and forth lines coming from $x = n_r - n_l = 2n_r - N$. Since $\sigma^2 = \langle x^2 \rangle - \langle x \rangle^2$, we can subtract $\langle x \rangle^2$ from both sides of (16) to get[2]

$$\sigma^2 = 4Np_r p_l \tag{17}$$

This is the distribution's variance, and is useful because it tells us that

$$\sigma \sim \sqrt{N} \tag{18}$$

which means that the particle in a classical random walk has an expected distance $O(\sqrt{N})$ from the origin.

[2]It's worth mentioning that in its usual application, a binomial distribution with parameters N, p_r has a an expectation Np_r and variance $Np_r p_l$ (which might be better expressed as $(\sqrt{N})^2 p_r p_l$ for comparison with (17)), but is defined for a distribution that is nonzero over $[0, N]$. In contrast, the classical random walk presented here has a distribution that is nonzero over $[-N, N]$, which is why (15) and(17) take a slightly different form than that for the more standard binomial distribution.

1.3.1 Biased random walks

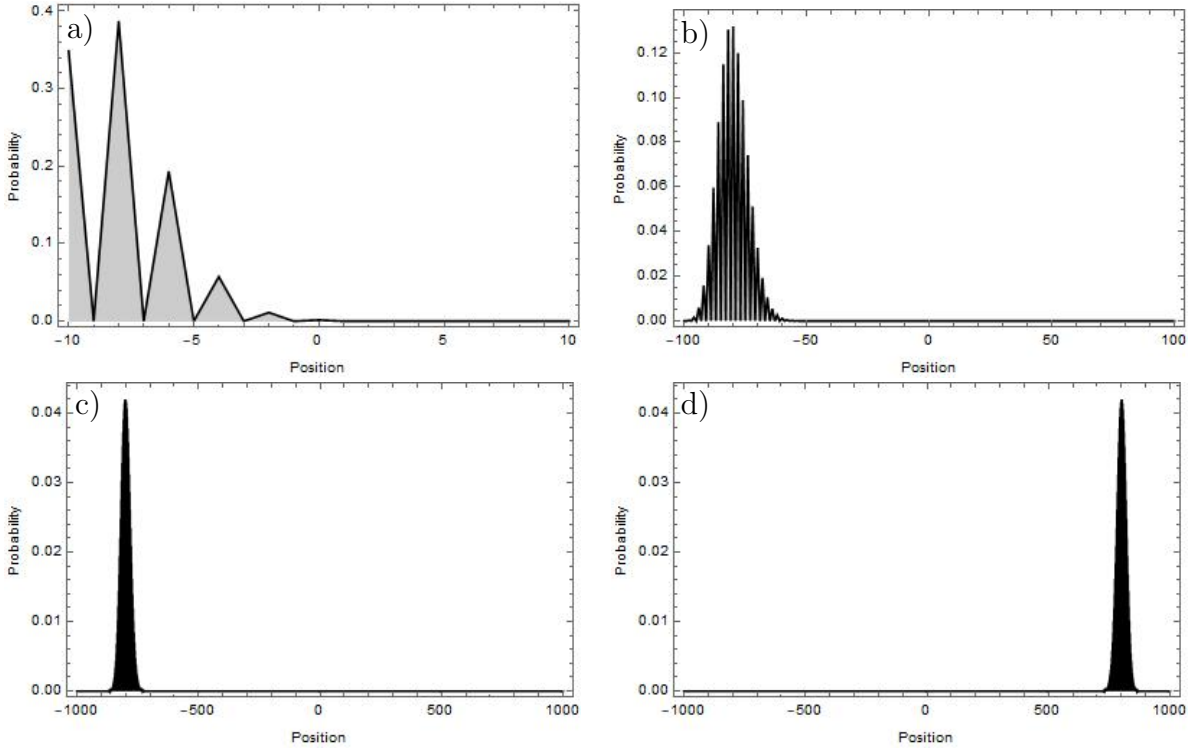

Figure 2: Distributions of a classical random walk, with $p_r = 0.1$, $N = 10, 100, 1000$ for Figures 2a,b,c. Figure 2d has $p_r = 0.9$ and $N = 1000$.

Figures 2a,b,c shows the probability distributions for the position of a particle in a classical random walk after $N = 10, 100$, and 1000 steps with $p_r = 0.1$. Figure 2d shows the probability distribution for a classical random walk with $N = 1000$ and $p_r = 0.9$. Figures 2a,b,c show that the distribution appears to become more normal with increasing N for constant $p_r = 0.1$, which is consistent with what the central limit theorem tells us should happen.

Figures 2c,d show that interchanging the values of p_r and p_l with fixed N has the effect of reflecting the distribution about the origin. This observation is consistent with $\langle x \rangle = N(p_r - p_l)$, which tells us that interchanging the values of p_r and p_l flips the sign on $\langle x \rangle$. It can also be discerned from looking at Figures 2c,d that interchanging p_r and p_l does not change the distribution's shape, which is consistent with the fact that $\sigma^2 = 4Np_rp_l$ remains unchanged when p_r and p_l are interchanged. The appearance of each distribution in Figure 2 appears to be consistent with (18), which tells us that the particle's expected distance from the origin grows as $O(\sqrt{N})$.

1.3.2 Going continuous with the gamma function

Before moving on to the idea of the continuous limit of a random walk on a line, it's worth noting that the distribution shown in Figure 1 can be made continuous by using the gamma function.

The gamma function

$$\begin{aligned}\Gamma(x) &= (x-1)! \\ &= \int_0^\infty y^{x-1}e^{-y}dy\end{aligned} \tag{19}$$

can be used to give us the notion of a continuous factorial. The fact that (19) is equivalent to the standard definition of a factorial for non-negative integer values of x, can be used to replace the factorials of the binomial coefficients in (4)

$$\binom{N}{n_r} = \frac{N!}{n_r!\,(N-n_r)!} \tag{20}$$

with gamma functions

$$\binom{N}{n_r} = \frac{\Gamma(N+1)}{\Gamma(n_r+1)\,\Gamma(N-n_r+1)} \tag{21}$$

This can be re-expressed as a function of position using $n_r(x) = \frac{1}{2}(x+N)$ from (3). Replacing the binomial coefficients in (4) with the expression in (20) allows us to re-write (4) as

$$P(x,N) = f\left(\tfrac{1}{2}(x+N)\right) \tag{22}$$

with f as it was defined in (4). I've used $P(\cdot)$ here, instead of $Prob(\cdot)$ to indicate that (22) is a probability density function, instead of a probability mass function, since replacing discrete point labels with continuous distance measures turned the probability mass function into a probability density function.

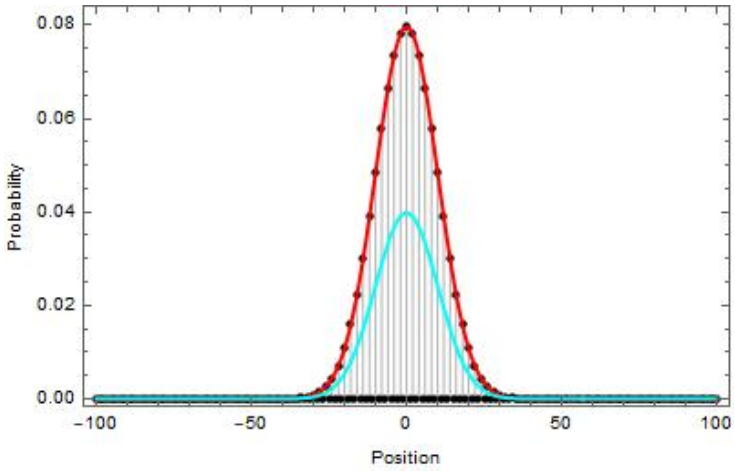

Figure 3: The gamma-function-continuous version of a classical random walk on a line (red), and its normalized-to-1 version (cyan), superimposed on top of the discrete classical random walk on a line that is shown in Figure 3 (black). The parameters used for three graphs are $N = 100, p_r = \frac{1}{2}$. This figure makes visual the fact that simply replacing the binomial coefficients with their corresponding gamma functions creates a distribution that exactly overlaps the probability mass points of the DTRW distribution, but does not accurately represent the continuous limit since it encloses twice the area of a CTRW (shown in Figure 6). However, when normalized to 1, the gamma-function-continuous version of a DTRW exactly overlaps the distribution of the actual continuous limit.

The gamma-function-continuous classical random walk is shown as the red curve in Figure 3. This curve exactly coincides with the probability mass points of the discrete classical random walk in Figure 1, which is plotted beneath it in Figure 3. Although this might seem like a good thing, it actually is not what we want. An easy way to see this is to integrate the area under the curve

$$\int_{-\infty}^{\infty} P\left(x, N \geq 1\right) dx = 2 \tag{23}$$

and we find that the distribution is not properly normalized. This integral can be calculated using computational software with (21) being used to replace the binomial coefficients in (2). If we renormalize the distribution, by dividing (22) by 2

$$P\left(x, N\right) = \frac{1}{2} f\left(\tfrac{1}{2}\left(x + N\right)\right) \tag{24}$$

we get the cyan-colored curve that is shown in Figure 3, which does not coincide with the probability mass points of the underlying discrete classical random walk distribution. The fact that the gamma-function-continuous version of a classical random walk on a line is normalized to 2 instead of 1, is one indication that replacing the binomial coefficients with their corresponding gamma functions is not the correct approach to modeling a classical random walk on a line as a continuous process. One explanation for why the gamma-function-continuous distribution encloses twice the area that you might expect, has to do

with the fact that all probability mass points in the discrete distribution are zero for either all odd or all even total numbers of steps N, as was discussed in the caption of Figure 1.

1.4 Continuous Limit of a Classical Random Walk on a Line

In this section we change notation from $Prob(\cdot) \to P(\cdot)$ since the function appears a lot. The derivation in this section draws primarily from [3, 6–9].

A discrete random walk on a line can be made continuous in space and/or time by taking the limit as the lattice spacing l and/or time step τ goes to zero. In this derivation we'll take both limits.

Assume that the particle is to located at position $x = i$ immediately following the N^{th} step. Then we know that at the beginning of its N^{th} step, the particle was either at $x = i-1$ and stepped right, or was at $x = i+1$ and stepped left. Since total probability is conserved, the probability $P(i, N)$ for the particle to be at $x = i$ immediately following its N^{th} step, must be equal to the sum of probabilities that flowed into $x = i$ on the N^{th} step. The probability for the particle to be at position $x = i - 1$ immediately before taking its N^{th} step is $P(i-1, N-1)$, and the probability that it stepped rightward on its N^{th} step is p_r. The probability of both of these events taking place is $p_r P(i-1, N-1)$. Similarly, the probability that the particle stepped left from $x = i + 1$ to $x = i$, on its N^{th} step is $p_l P(x+1, N-1)$. Then the sum of probabilities that flow into $x = i$ on the N^{th} step is

$$P(i, N) = p_r P(i-1, N-1) + p_l P(i+1, N-1) \tag{25}$$

This condition on the particle's time evolution can be turned into a difference quotient, which is then turned into a differential equation in the large N limit (continuous limit), which can then be solved to find the function that governs the particle's time evolution.

The discrete variables i, N that we have been using so far are just the labels that we have used to name specific points along the space and time axes. Using these labels made sense for the discrete time random walk because all of the points had a constant finite distance between them, so we could easily attribute a numerical distance that they represent by multiplying the distance between adjacent points back in, $x = il$, $t = N\tau$. An important technical point, is that $x = x(i)$ and $t = t(N)$ are discrete variables at this point, whose values are determined by i, N. x, t do not actually become continuous variables until we take the limit $l, \tau \to 0$.

Taking the continuous limit is done by taking the limit as the distance between neighboring points goes to zero $l, \tau \to 0$. In doing this, finite distances of the particle from the origin, and of time since the start of the random walk, correspond to arbitrarily large values of i, N, since it takes a lot of infinitesimal i, N to create a finite distance. So any realistic case of (25) that we might want to consider becomes $P(i \to \infty, N \to \infty)$ in the continuous limit. In order for (25) to still be meaningful after we take the continuous limit, we need to rewrite in terms of variables that remain finite throughout the course of the random walk. Substituting $i = \frac{x}{l}$ and $N = \frac{t}{\tau}$ in (25),

$$P\left(\frac{x}{l},\frac{t}{\tau}\right)=p_rP\left(\frac{x}{l}-1,\frac{t}{\tau}-1\right)+p_lP\left(\frac{x}{l}+1,\frac{t}{\tau}-1\right) \tag{26}$$

We can now change the units of each argument in (26) $\frac{x}{l}\to x,\frac{t}{\tau}\to t$, since our choice of units does not affect the validity of the equation

$$P\left(x,t\right)=p_rP\left(x-l,t-\tau\right)+p_lP\left(x+l,t-\tau\right) \tag{27}$$

This step was important, because now the arguments of the probability function will remain finite when we take the limits $l,\tau\to 0$.

We can set up a difference quotient for the rate of change of $P(x,t)$ with respect to time by dividing both sides of (27) by τ, subtracting $P(x,t-\tau)/\tau$ from both sides, and then using $p_r+p_l=1$ on the right hand side of the resulting equation to turn each term into a difference quotient

$$\frac{P(x,t)-P(x,t-\tau)}{\tau}=p_r\frac{P(x-l,t-\tau)-P(x,t-\tau)}{\tau}+p_l\frac{P(x+l,t-\tau)-P(x,t-\tau)}{\tau} \tag{28}$$

We can use the constraint that total probability must equal one to eliminate a parameter. Using $p_r+p_l=1=1/2+1/2+\varepsilon-\varepsilon$, which is satisfied by

$$p_r=1/2+\varepsilon\quad\text{and}\quad p_r=1/2-\varepsilon \tag{29}$$

for some ε. Making this substitution into (28) allows us to write

$$\begin{aligned}\frac{P(x,t)-P(x,t-\tau)}{\tau}=&\frac{1}{2}\left(\frac{P(x-l,t-\tau)-P(x,t-\tau)}{\tau}+\frac{P(x+l,t-\tau)-P(x,t-\tau)}{\tau}\right)\\&+\varepsilon\left(\frac{P(x-l,t-\tau)-P(x,t-\tau)}{\tau}-\frac{P(x+l,t-\tau)-P(x,t-\tau)}{\tau}\right)\end{aligned} \tag{30}$$

When we take the limit $\tau\to 0$ the left hand side of (30) will become $\frac{P(x,t)-P(x,t-\tau)}{\tau}\to\frac{\partial P(x,t)}{\partial t}$. We need to do some work on the right hand side of the equation so that we can see that it will also converge to a partial derivative when we take $l,\tau\to 0$.

Taylor expanding $P(x,t-\tau)$ in powers of $t-\tau$ about the point (x,t) results in a canceling out of t that leaves us with a power series in τ. Expanding the series to its first non-vanishing order in τ gives,

$$\begin{aligned}P(x,t-\tau)\Big|_{\substack{\text{expanded}\\\text{about }(x,t)}}&=\sum_{n=0}^{\infty}\frac{1}{n!}\frac{\partial^nP\left(x,t\right)}{\partial\left(t-\tau\right)^n}\left(t-\tau-t\right)^n\\&=P(x,t)-\frac{\partial P(x,t)}{\partial\left(t-\tau\right)}\tau+\mathcal{O}\left(\tau^2\right)\end{aligned} \tag{31}$$

Expansion about (x,t) in powers of $t-\tau$ assumes that the only variable parameter in (31) is τ. So the function itself, on the left hand side, should be thought of as $P\colon \tau \to [0,1]$ for the time being.

When expanding $P(x \pm l, t-\tau)$ about (x,t) in orders of $x \pm l, t-\tau$, we are required to expand to the second non-vanishing order in l, since the terms that are first order in l will cancel each other out when the Taylor expansions are used to reconstruct the right hand side of (30). Expanding $P(x \pm l, t-\tau)$ about (x,t)

$$\begin{aligned} P(x \pm l, t-\tau)\Big|_{\substack{\text{expanded} \\ \text{about } (x,t)}} &= P(x,t) - \frac{\partial P(x,t)}{\partial\,(t-\tau)}\tau \pm \frac{\partial P(x,t)}{\partial(x \pm l)}l + \frac{1}{2}\frac{\partial^2 P(x,t)}{\partial(x \pm l)^2}l^2 \\ &\quad + \mathcal{O}\left(\tau^2\right) + \mathcal{O}\left(\tau l\right) + \mathcal{O}\left(l^3\right) \end{aligned} \tag{32}$$

Subtracting (31) from (32), dropping the higher order terms, dividing both sides by τ, and using the result to replace each difference quotient on the right hand side of (30) gives,

$$\frac{P(x,t) - P(x,t-\tau)}{\tau} = \frac{1}{4}\frac{l^2}{\tau}\left[\frac{\partial^2 P(x,t)}{\partial(x-l)^2} + \frac{\partial^2 P(x,t)}{\partial(x+l)^2}\right] - \varepsilon\frac{l}{\tau}\frac{\partial P(x,t)}{\partial(x-l)} \tag{33}$$

Now we can take $\varepsilon \to 0$ to eliminate the the first order partial derivative,

$$\frac{P(x,t) - P(x,t-\tau)}{\tau} = \frac{1}{4}\frac{l^2}{\tau}\left[\frac{\partial^2 P(x,t)}{\partial(x-l)^2} + \frac{\partial^2 P(x,t)}{\partial(x+l)^2}\right] \tag{34}$$

Note from (29) that this commits use to an unbiased random walk, since we're now assuming equal probabilities for moving right and left on each step. Taking the limit $l, \tau \to 0$ such that $\alpha \equiv \frac{l^2}{2\tau}$ remains finite gives

$$\frac{\partial P(x,t)}{\partial t} = \alpha\frac{\partial^2 P(x,t)}{\partial x^2} \tag{35}$$

This means that the continuous limit of a classical random walk on a line is described by the heat/diffusion equation, which can be solved using the convolution theorem for Fourier transforms.

Applying a Fourier transformation $P\,(x,t) \to \widehat{P}\,(k,t)$, with the hat denoting the Fourier transformed function, to both sides of (35). On the left hand side

$$\begin{aligned} \widehat{P}_t(k,t) &= \frac{1}{\sqrt{2\pi}}\int_{-\infty}^{\infty}\frac{\partial P(x,t)}{\partial t}e^{-ikx}dx \\ &= \frac{\partial}{\partial t}\left(\frac{1}{\sqrt{2\pi}}\int_{-\infty}^{\infty}P(x,t)e^{-ikx}dx\right) \\ &= \frac{\partial}{\partial t}\widehat{P}(k,t) \end{aligned} \tag{36}$$

Fourier transforming the right hand side of (35), and then using integration by parts $f'g = (fg)' - fg'$ to rewrite it as a sum of two integrals

$$\begin{aligned}
\alpha\widehat{P_{xx}}(k,t) &= \frac{1}{\sqrt{2\pi}}\int_{-\infty}^{\infty}\left(\alpha\frac{\partial^2 P(x,t)}{\partial x^2}\right)e^{-ikx}dx \\
&= \frac{\alpha}{\sqrt{2\pi}}\int_{-\infty}^{\infty}\frac{\partial}{\partial x}\left(P_x(x,t)e^{-ikx}\right)dx - \frac{\alpha}{\sqrt{2\pi}}\int_{-\infty}^{\infty}P_x(x,t)\frac{\partial}{\partial x}e^{-ikx}dx \\
&= \left(P_x(x,t)e^{-ikx}\right)\Big|_{x=-\infty}^{\infty} + \frac{ik\alpha}{\sqrt{2\pi}}\int_{-\infty}^{\infty}P_x(x,t)e^{-ikx}dx \\
&= \frac{ik\alpha}{\sqrt{2\pi}}\int_{-\infty}^{\infty}P_x(x,t)e^{-ikx}dx \qquad (37)
\end{aligned}$$

The boundary term in the third line vanishes since $P(x,t)$ must go to zero at $x = \pm\infty$, since total probability is equal to one. The fact that $P(x,t)$ becomes arbitrarily small as $x \to \infty$ also means that it becomes arbitrarily constant (equal to zero) as $x \to \infty$. So $P_x(x = \pm\infty, t) = 0$ is required in order for $P(x,t)$ to be convergent.

Applying integration by parts a second time,

$$\begin{aligned}
\alpha\widehat{P_{xx}}(k,t) &= \frac{ik\alpha}{\sqrt{2\pi}}\int_{-\infty}^{\infty}\frac{\partial}{\partial x}\left(P(x,t)e^{-ikx}\right)dx - \frac{k^2\alpha}{\sqrt{2\pi}}\int_{-\infty}^{\infty}P(x,t)e^{-ikx}dx \\
&= -\frac{k^2\alpha}{\sqrt{2\pi}}\int_{-\infty}^{\infty}P(x,t)e^{-ikx}dx \\
&= -k^2\alpha\widehat{P}(k,t) \qquad (38)
\end{aligned}$$

Putting the results of (36),(38) into a Fourier transformed version of (35) simplifies the PDE into a first-order ODE over time in Fourier space

$$\frac{\partial}{\partial t}\widehat{P}(k,t) = -\alpha k^2\widehat{P}(k,t) \qquad (39)$$

which gives us a function $\widehat{P}(k,t)$ whose time-derivative is proportional to itself, by a constant factor $-\alpha k^2$. We therefore have the solution

$$\widehat{P}(k,t) = \widehat{P}(k,0)e^{-\alpha k^2 t} \qquad (40)$$

The fact that $\widehat{P}(k,t)$ is equal to a product of two functions of k, suggests that it may be solvable using the convolution theorem for Fourier transforms. The convolution theorem for Fourier transforms states that for two functions $f(x), g(x)$, their convolution

$$(f * g)(x) = \frac{1}{\sqrt{2\pi}}\int_{-\infty}^{\infty} f(\xi)\, g(x-\xi)\, d\xi, \qquad (41)$$

has a Fourier transform that is equal to the product of the two function's individual Fourier transforms

$$\widehat{(f*g)}(k) = \widehat{f}(k)\,\widehat{g}(k) \tag{42}$$

This means that if we have a Fourier transformed function $\widehat{h}(k)$, that can be written as a product of two separable functions of k, $\widehat{h}(k) = \widehat{f}(k)\,\widehat{g}(k)$, rather than calculating the inverse Fourier transform for the right hand side directly, we can instead, calculate the inverse Fourier transforms $f(x) = F^{-1}\widehat{f}(k)$ and $g(x) = F^{-1}\widehat{g}(k)$ separately, and then put $f(x), g(x)$ into (41) to get $h(x)$ indirectly

$$\begin{aligned} h(x) &= F^{-1}\widehat{h}(k) \\ &= \widehat{(f*g)}(x) \end{aligned} \tag{43}$$

Applying the convolution theorem to (40), let $\widehat{f}(k) = \widehat{P}(k,0)$ and $\widehat{g}(k) = e^{-\alpha k^2 t}$. Then the convolution theorem tells us that $P(x,t) = F^{-1}\widehat{P}(k,t) = \widehat{(f*g)}(x)$. This means

$$\begin{aligned} f(x) &= F^{-1}\widehat{P}(k,0) \\ &= P(x,t) \end{aligned} \tag{44a}$$

$$\begin{aligned} g(x) &= F^{-1}e^{-k^2\alpha t} \\ &= \frac{1}{\sqrt{2\pi}}\int_{-\infty}^{\infty} e^{-k^2\alpha t + ikx}dk \end{aligned} \tag{44b}$$

This integral can be turned into a Gaussian by completing the square in the exponent. Let $a = \sqrt{\alpha t}k$ and $2ab = ikx$. This allows us to complete the square as $(a-b)^2 - b^2$ with $b = \frac{ix}{2\sqrt{\alpha t}}$.

$$\begin{aligned} g(x) &= \frac{1}{\sqrt{2\pi\alpha t}}\int_{-\infty}^{\infty} e^{-(a-b)^2+b^2}da \\ &= \frac{1}{\sqrt{2\alpha t}}e^{-x^2/(4\alpha t)} \end{aligned} \tag{45}$$

which is easily evaluated using $\int_{-\infty}^{\infty} e^{-(a-b)^2}da = \sqrt{\pi}$. Putting (44a) and (45) into (41) and using the convolution theorem for Fourier transforms, which tells us that $P(x,t) = F^{-1}\widehat{P}(k,t) = \widehat{(f*g)}(x)$, with $\widehat{(f*g)}(x)$ given by (42)

$$\begin{aligned} P(x,t) &= \frac{1}{\sqrt{2\pi}}\int_{-\infty}^{\infty} f(\xi)g(x-\xi)d\xi \\ &= \frac{1}{\sqrt{4\pi\alpha t}}\int_{-\infty}^{\infty} P(\xi,0)e^{-(x-\xi)^2/(4\alpha t)}d\xi \end{aligned} \tag{46}$$

At time $t = 0$ there is a 100% probability that the particle will be located at $x = 0$. In going from (26) to (27), we changed from a probability mass function into a probability density function. Since the particle is exactly located at $x = 0$ at time $t = 0$, we have

$$P(x,0) = \begin{cases} \infty & \text{if } x = 0 \\ 0 & \text{otherwise} \end{cases} \tag{47}$$

which means $P(x,0) = \delta(x)$. So (46) becomes,

$$P(x,t) = \frac{1}{\sqrt{4\pi\alpha t}} \int_{-\infty}^{\infty} \delta(\xi) e^{-(x-\xi)^2/(4\alpha t)} d\xi \tag{48}$$

Evaluating the integral, we have

$$P(x,t) = \frac{1}{\sqrt{4\pi\alpha t}} e^{-x^2/(4\alpha t)} \tag{49}$$

$P(x,t)$ is normally distributed with parameters $\mu = 0$ and $\sigma^2 = 2\alpha t$. A normal distribution is what we should expect, since the binomial distribution converges to a normal distribution in the large N limit.

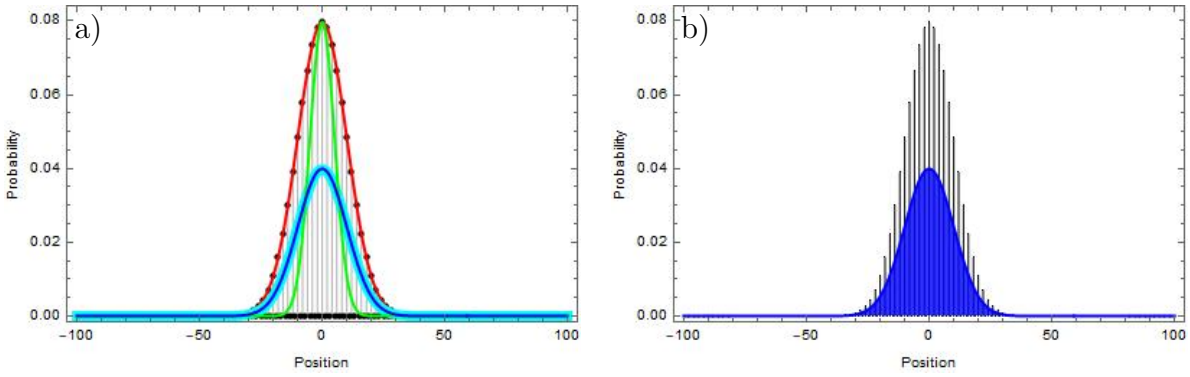

Figure 4: All DTRWs shown have parameters $N = 100, p_r = 1/2$. In Figure 4a: the black dots are the probability mass points from the random walk in Figure 1, the red curve is the un-normalized gamma-function-continuous version of an unbiased DTRW from Section 1.3.2, the cyan-colored curve is the normalized gamma-function-continuous version from Section 1.3.2, the green curve is the distribution for a CTRW with $\alpha = 0.12563$, and the blue curve is the the distribution for the continuous limit for $\alpha = 1/2$. The green curve shows that when $\alpha = 0.12563$, the continuous limit of a random walk has an expected distance from the origin $\sigma \approx 5$, which attains the same maximum height as the DTRW from Figure 1. The blue curve shows that for the special case $\alpha = 1/2$, the continuous limit completely overlaps the normalized gamma-function-continuous version. In Figure 6b: the distribution for the continuous limit (blue) is superimposed on top of the distribution for the discrete case (black). Both distributions are normalized to 1, but the particle in a DTRW can only access even/odd x positions, depending on the parity of the number of time steps N. The result of this is that its distribution takes alternative steps between zero and nonzero probability as you move from left to right across the distribution. Both graphs enclose the same amount of total area.

Curves representing CTRWs with $\alpha = 0.12563$ and $\alpha = 0.5$ are shown in green and blue in Figure 4a. These curves both have a variance $\sigma^2 = 2\alpha t = 25.1253$, while the DTRW distribution, depicted as black dots in Figure 4a, has a variance of $\sigma^2 = 4Np_rp_l = 100$. This difference can be attributed to the parameter $\alpha \equiv \frac{l^2}{2\tau}$, which from (35), determines the comparative sizes of the scaling between position and time parameters.

1.5 Classical Random Walk in Higher Dimensions

This example is based primariloy off of [6]. A classical random walk on a line can be extended to a classical walk in a higher dimensions by representing the particle's spatial probability distribution as a multinomial distribution, with its number of categories equal to twice the number of spatial dimensions the particle has to move in. Twice, because during each time step, the particle moves in one of two directions along each spatial dimension. So a DTRW in d spatial dimensions can be modeled as a multinomial distribution with $2d$ categories.[3]

In this section, we will find the probability distribution for a classical DTRW in two spatial dimensions. Two spatial dimensions means that on any given time step, the particle can move in one of four possible directions x_+, x_-, y_+, y_-. Throughout the duration of the random walk, the number of steps the particle has taken in each of the four directions (two directions along each dimension) is kept track of using the parameters n_1, n_2, n_3, n_4, respectively. The particle steps in these directions with corresponding probabilities p_1, p_2, p_3, p_4, which are subject to the constraints

$$p_1 + p_2 + p_3 + p_4 = 1 \tag{50a}$$
$$n_1 + n_2 + n_3 + n_4 = N \tag{50b}$$

where as before, N is the total number of time steps, which is equal to the total number of steps the particle has taken.

The particle's initial position is at the origin. Since each step is modeled as an independent event, the probability that the particle will take any one path that has exactly n_1, n_2, n_3, and n_4 steps along their corresponding directions, is equal to

$$p_1{}^{n_1} p_2{}^{n_2} p_3{}^{n_3} p_4{}^{n_4} \tag{51}$$

And for a given specification of n_1, n_2, n_3, and n_4, there are

$$\binom{N}{n_1, n_2, n_3, n_4} = \frac{N!}{n_1! n_2! n_3! n_4!} \tag{52}$$

distinct N-step paths the particle can take to get to its final position $(x, y) = (i, j)$.

[3] It's worth noting that for the special case of one spatial dimension, the multinomial distribution reduces to a binomial distribution, which is consistent with what we were working with in the previous sections.

With all of this taken into account, the probability that a particle will distribute its N steps as n_1, n_2, n_3, n_4 is

$$Prob\left(X_+ = n_1, X_- = n_2, Y_+ = n_3, Y_- = n_4\right) = \binom{N}{n_1, n_2, n_3, n_4} {p_1}^{n_1} {p_2}^{n_2} {p_3}^{n_3} {p_4}^{n_4} \tag{53}$$

where X_+, X_-, Y_+, Y_- are random variables representing the number of steps taken in their indicated directions. The particle's position after taking its N^{th} step is given by

$$(x, y) = (n_1 - n_2, n_3 - n_4) \tag{54}$$

As was the case in formulating a DTRW in one dimension, we would like to have a probability mass function that we can specify a position $(x, y) = (i, j)$, and number of time steps N for, and be given the probability that the particle will be at that position at the end of its N^{th} step. To get such a function, we want to replace parameters n_1, n_2, n_3, n_4 in (53) that we don't care about being able to specify, with relations that express them in terms of the parameters that we do care about being able to specify x, y, N, when plotting the distribution.

We can use (50b), (54) to help us eliminate some degrees of freedom, by using them to build a system of linear equations that is underdetermined by one equation when we treat x, y, N as knowns. From (50b), (54)

$$n_1 - n_2 = x \tag{55a}$$
$$n_3 - n_4 = y \tag{55b}$$
$$n_1 + n_2 + n_3 + n_4 = N \tag{55c}$$

which can be solved to give

$$n_1 = f_1(N, x, y, n_4) = \tfrac{1}{2}(N + x - y) - n_4 \tag{56a}$$
$$n_2 = f_2(N, x, y, n_4) = \tfrac{1}{2}(N - x - y) - n_4 \tag{56b}$$
$$n_3 = f_3(y, n_4) = y + n_4 \tag{56c}$$
$$n_4 = n_4 \tag{56d}$$

Substituting each of these equations into (53) and replacing x, y by their discrete-value equivalents i, j gives,

$$Prob\left[(x, y) = (i, j), N\right] = \sum_{n_4=0}^{N} f\left(i, j, N, n_4\right) \tag{57}$$

where

$$f\left(i,j,N,n_4\right)=\binom{}{f_1(N,i,j,n_4),\,f_2(N,i,j,n_4),\,f_3(j,n_4),\,n_4}{p_1}^{f_1(N,i,j,n_4)}{p_2}^{f_2(N,i,j,n_4)}{p_3}^{f_3(j,n_4)}{p_4}^{n_4} \tag{58}$$

$f\left(i,j,N,n_4\right)$ gives the conditional probability for the particle to land at (x,y) on its N^{th} step, given that it takes a fixed number of steps n_4 in the $-\hat{\boldsymbol{y}}$-direction. The summation over n_4 sums over all possible paths the particle can take to get to $(x,y)=(i,j)$ on its N^{th} step, with $f(i,j,N,n_4)$ representing the total probability for all paths that have the same values for n_4. It's worth noting that p_1,p_2,p_3,p_4 are treated as predetermined constants in this equation.

1.5.1 Conditions

The condition that n_1,n_2,n_3,n_4 are non-negative integers, which is imposed by their definition, indirectly imposes conditions on what combinations of x,y,N,n_4 correspond to possible paths the particle can take. For example, $(x,y,N,n_r)=(2,1,4,1)$ does not represent a valid combination of parameters because (56a) tells us that it would mean $n_1=\frac{5}{2}$. To plot the distribution, we can have the plotting process iterate through all possible combinations of (x,y,N,n_4) for a chosen fixed value of N, and n_4 as all integers in $[0,N]$, and on each iteration, use conditions on (x,y,N,n_4) to throw out the paths that are not possible for the particle to take. We need to impose conditions to guarantee that n_1,n_2,n_3 are always integers, and are always non-negative.

First, we can impose the condition that n_1,n_2 only be allowed to take on integer values, by imposing conditions on allowable combinations of x,y,N. Since $n_1=\frac{1}{2}\left(N+x-y\right)-n_4$ and $n_2=\frac{1}{2}\left(N-x-y\right)-n_4$, and we are able to manually specify n_4 as an integer (by telling the software to iterate through $n_4\in[0,N]$), we know that $\frac{1}{2}\left(N+x-y\right)$ must also be an integer in order for n_1,n_2 to be integers. So we can require

$$\tfrac{1}{2}\left(N\pm x-y\right)\mod 1=0 \tag{59}$$

No constraint is needed to guarantee that n_3 only takes on integer values, since $n_3=y+n_4$, and the fact that y and n_4 are both defined as integers means that n_3 is also an integer.

Second, to ensure $n_1,n_2\geq 0$ we can use

$$\tfrac{1}{2}\left(N\pm x-y\right)-n_4\geq 0 \tag{60}$$

Third, $n_3=y+n_4$ means that n_3 takes on negative values whenever $n_4>-y$. To prevent n_3 from taking on negative values we can require

$$n_4\geq -y \tag{61}$$

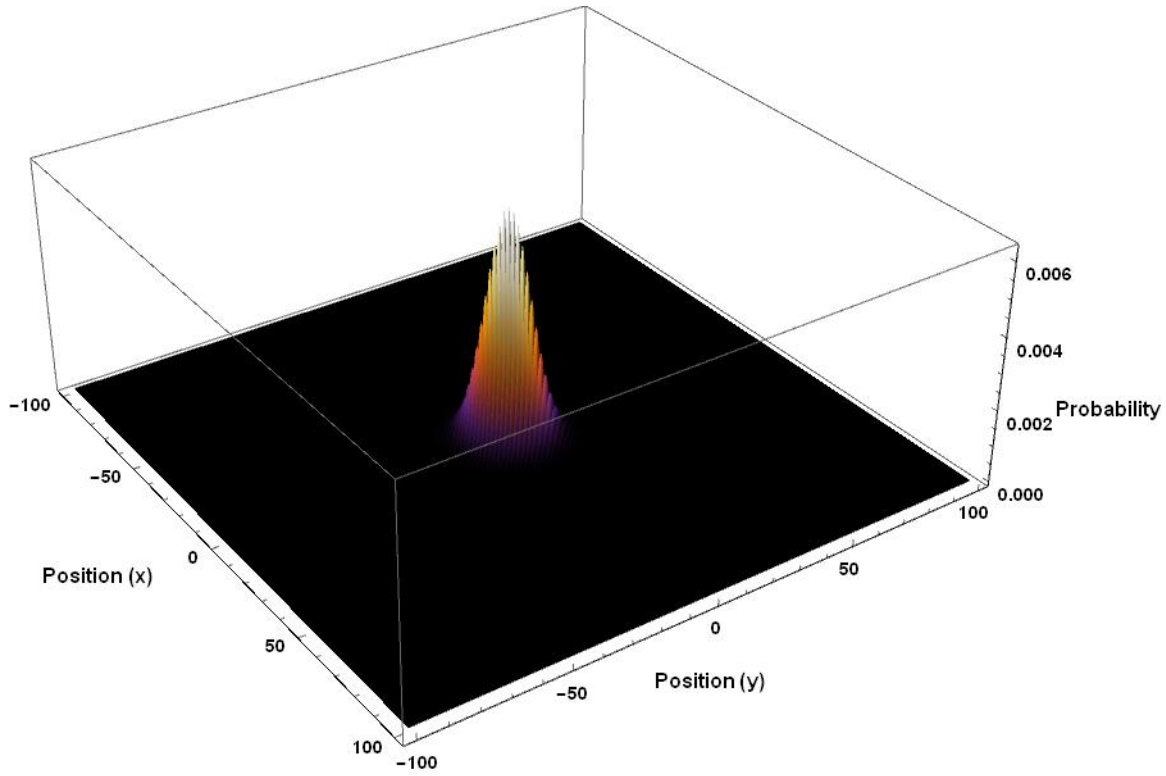

Figure 5: Distribution of an unbiased 2-dimensional classical random walk after $N = 100$ steps.

An important feature of the two-dimensional distribution, which was also true of the one-dimensional distribution, is that after a given number of steps N, there will always be a set of positions that the particle has zero probability of being located at immediately after its N^{th} step. For example, there is no path that has an odd number of steps that ends at $(x, y) = (0, 0)$. This fact is depicted visually in Figure 5 by the lack of smoothness in the distribution when one looks at it closely.

As shown in Figure 5, 100 steps of the random walk demonstrates that the distribution is normal. The expectation value for the particles position is given by

$$\begin{aligned}\langle \boldsymbol{r} \rangle &= \sum_{i=1}^{4} \langle x_i \rangle \, \hat{\boldsymbol{\imath}} \\ &= \sum_{i=1}^{4} N p_r \hat{\hat{\boldsymbol{\imath}}} \\ &= N \left[p_1 \hat{\boldsymbol{x}} + p_2 \left(-\hat{\boldsymbol{x}} \right) + p_3 \hat{\boldsymbol{y}} + p_4 \left(-\hat{\boldsymbol{y}} \right) \right] \end{aligned} \tag{62}$$

Therefore,

$$\langle \boldsymbol{r} \rangle = N(p_1 - p_2)\hat{\boldsymbol{x}} + N(p_3 - p_4)\hat{\boldsymbol{y}} \tag{63}$$

(63) has the same functional form in each of its components as (9), the position expectation for a random walk on a line. Similarly, the variance in the particles position along each spatial axis can be shown to be ${\sigma_i}^2 = 4Np_{i_+}\left(1 - p_{i_+}\right)$ for $i \in \{x, y\}$, and the + subscript indicates movement along the positive direction of the given axis. So the variance also has an equivalent functional form in each of its components, to the variance that was found for a random walk on a line (17).

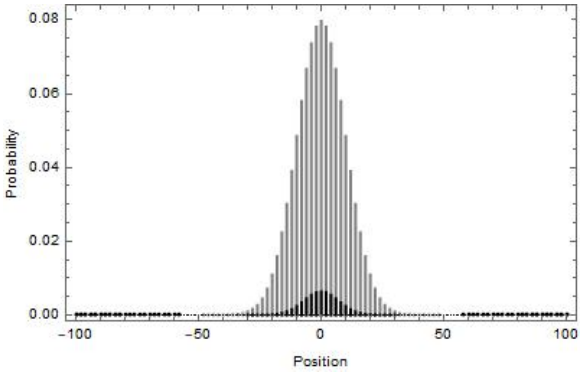

Figure 6: Cross section along $y = 0$ of a random walk in two spatial dimensions, superimposed on top of the distribution for a random walk in 1 dimension. Adding extra spatial dimensions causes the distribution's cross section to become smaller, since the probability density has a lot more positions to distribute itself among in higher spatial dimensions.

However, with more spatial dimensions, the magnitude of the variance is smaller along each dimension, since the total probability weight that each p_{i_+} represents decreases with increasing dimensionality of the space, while total probability remains 1. This decrease in the variance that accompanies additional spatial dimensions is shown in Figure 6, which superimposes the cross section of a two-dimensional random walk's distribution on top of the distribution for a random walk on a line.

2 Part 2: Quantum Random Walks

A single-particle quantum walk on a line starts with a particle's wavefunction $|\Psi\rangle$ in an initial state $|\Psi_0\rangle$ that is a composite state of spin and position. For an example, we might start with

$$|\Psi_0\rangle = (\alpha_\uparrow |\uparrow\rangle + \alpha_\downarrow |\downarrow\rangle) \otimes |x_0\rangle \tag{64}$$

as the initial state. During each time step, the wavefunction is acted on by a suite of operations that together comprise the time evolution operator

$$U = S \cdot (C \otimes I) \tag{65}$$

The first operation $C \otimes I$ is applied at the beginning of each time step, and represents a rotation of the particle's spin component, which is enacted the by coin operator C. In classical physics, the particle moves either right or left during each time step. In quantum mechanics, the particle's wavefunction moves in a linear combination of both right and left. $C \otimes I$ acts like a coin, in that it mixes up the directions that the wavefunction's eigenstates are headed in at the beginning of each turn.

The second operation during each time step is performed by the conditional translation operator S, which translates each eigenstate either right or left, depending on whether the eigenstate is spin-up or spin-down.

The time step ends after both operations on the right-hand side of (65) have been enacted. At the end of each time step, a new one initiates, and the process is repeated until a total of N time steps have been completed.

2.1 The Hadamard Walk on a Line

The following is motivated by [1–3, 7, 11, 12]. The Hadamard walk on a line is a quantum walk, that uses the Hadamard coin

$$H = \frac{1}{\sqrt{2}} \begin{pmatrix} 1 & 1 \\ 1 & -1 \end{pmatrix} \tag{66}$$

as its coin operator. The action of $H \otimes I$ on the basis states of the particle's Hilbert space $\mathcal{H} = \mathcal{H}_C \otimes \mathcal{H}_P$ is,

$$|\uparrow\ i\rangle \to \frac{1}{\sqrt{2}} (|\uparrow\rangle + |\downarrow\rangle) \otimes |i\rangle \tag{67a}$$

$$|\downarrow\ i\rangle \to \frac{1}{\sqrt{2}} (|\uparrow\rangle - |\downarrow\rangle) \otimes |i\rangle \tag{67b}$$

The conditional translation operator S for this quantum walk is defined as

$$S = |\uparrow\rangle\langle\uparrow| \otimes \sum_{i=-\infty}^{\infty} |i+1\rangle\langle i| + |\downarrow\rangle\langle\downarrow| \otimes \sum_{i=-\infty}^{\infty} |i-1\rangle\langle i| \tag{68}$$

The action of S on the basis states of $\mathcal{H}$ is,

$$\begin{aligned} |\uparrow\ i\rangle &\to |\uparrow\ i+1\rangle \\ |\downarrow\ i\rangle &\to |\downarrow\ i-1\rangle \end{aligned}$$

The time evolution operator (65) that enacts each time step of the quantum walk is

$$U = S \cdot (H \otimes I) \tag{69}$$

which acts on the particle's wavefunction to propagate it through one time step.

To get a feel for how this works, consider a particle in the initial state

$$|\Psi_0\rangle = |\uparrow\ 0\rangle \tag{70}$$

To initiate the random walk we act on $|\Psi_0\rangle$ with U, which propagates the wavefunction through the first stroboscopic time step

$$\begin{aligned} |\Psi_1\rangle &= U|\Psi_0\rangle \\ &= S(H \otimes I)(|\uparrow\rangle \otimes |0\rangle) \\ &= S\frac{1}{\sqrt{2}}(|\uparrow\rangle + |\downarrow\rangle) \otimes |0\rangle \\ &= \frac{1}{\sqrt{2}}(|\uparrow\ 1\rangle + |\downarrow\ -1\rangle) \end{aligned} \tag{71}$$

If we iterate the quantum walk through two more time steps using repeated applications of U on $|\Psi_1\rangle$, without making any measurements between the two time steps, we get

$$|\Psi_2\rangle = \frac{1}{2}[|\uparrow\rangle \otimes (|2\rangle + |0\rangle) + |\downarrow\rangle \otimes (|0\rangle - |-2\rangle)] \tag{72a}$$

$$|\Psi_3\rangle = \frac{1}{\sqrt{2^3}}[|\uparrow\rangle \otimes (|3\rangle + 2|1\rangle - |-1\rangle) + |\downarrow\rangle \otimes (|1\rangle + |-3\rangle)] \tag{72b}$$

Quantum mechanics predicts that if we were to stop the quantum walk at this point and measure the particle's position, we would find the particle to be located at $x = -3, -1, 3$, each with probability $\frac{1}{8}$, or at $x = 1$ with probability $\frac{5}{8}$

$$|\langle x|\Psi\rangle|^2 = \begin{cases} \frac{1}{8} & \text{for } x = -3, -1, 3 \\ \frac{5}{8} & \text{for } x = 1 \end{cases} \tag{73}$$

If we were to let the quantum walk run through 100 time steps before measuring the particle's position, quantum mechanics predicts that we would find a probability distribution of its spatial location that looks like the one shown in Figure 7a.

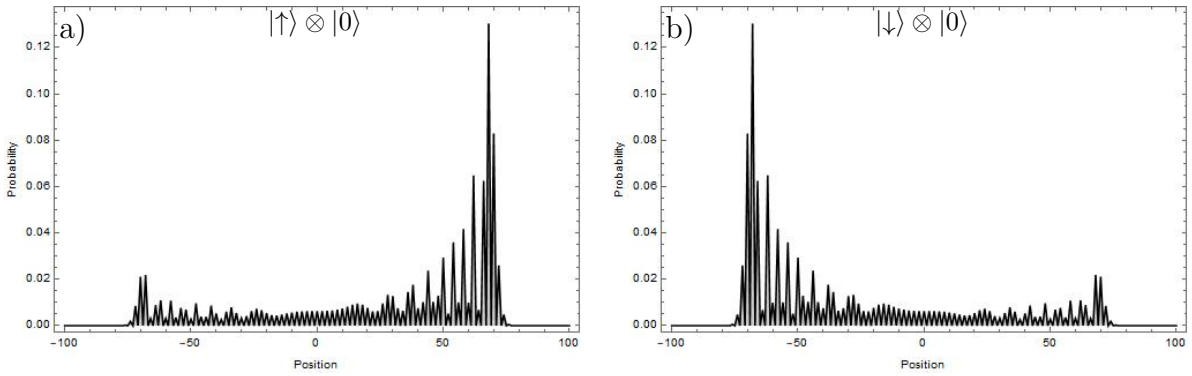

Figure 7: Simulations after 100-steps of a Hadamard walk on a line. Figure 7a,b were simulated using initial states $|\uparrow\ 0\rangle, |\downarrow\ 0\rangle$, respectively.

Figures 7a, 7b show simulations of the Hadamard walk on a line after 100 steps, using initial states $|\uparrow\ 0\rangle$ and $|\downarrow\ 0\rangle$, respectively. At a glance, the two distributions appear to be mirror reflections of each other about $x = 0$. However, this is not quite true. We can calculate moments of each distribution using

$$\langle x^n \rangle = \sum_{i=-N}^{N} i^n |\langle i\ |\Psi_N\rangle|^2 \tag{74}$$

and the variance using

$$\sigma^2 = \langle x^2 \rangle - \langle x \rangle^2 \tag{75}$$

The expectation and variance of the particle's position after 100 steps are shown in Table 1.

$\|\Psi_0\rangle$	$\langle x \rangle$	σ^2
$\|\uparrow\ 0\rangle$	29.9756	2928.93
$\|\downarrow\ 0\rangle$	-28.9756	2089.84
$\frac{1}{\sqrt{2}}(\|\uparrow\ 0\rangle + \|\downarrow\ 0\rangle)$	29.6427	2050.73
$\frac{1}{\sqrt{2}}(\|\uparrow\ 0\rangle + i\|\downarrow\ 0\rangle)$	0	2929.42

Table 1: Expectation and variance of the particle's position after 100 steps of a Hadamard walk for the simulations done in this section.

The distribution in Figure 7a has an expected position $\langle x \rangle = 29.9756$ and variance $\sigma^2 = 2,928.93$, while the distribution in Figure 7b has $\langle x \rangle = -28.9756$ and $\sigma^2 = 2,089.84$.

The visual difference betwen the two simulations in Figure 7 shows that changing particle's initial state can have a dramatic impact on the outcome of the quantum walk. This ability to change the outcome of the distribution by changing the particle's initial state is a feature that is unique to quantum random walks, and has no analog in the formulation of classical random walks.

The expectation and variance of the position of a classical particle in an unbiased random walk starting at $x = 0$, are $\langle x \rangle = 0$ and $\sigma^2 = 100$, from (9) and (17). Comparison of these values to what was found for the two quantum walk simulations above demonstrates the tendency of the particle in a quantum walk to increase its expected distance from the distribution's center σ much faster than for a classical random walk. The variance of quantum random walks has been found to increase with the number of time steps as $O(N)$, which is quadratically faster than the what was found for classical random walks $O(\sqrt{N})$ [2].

Unlike the classical random walk shown in Figure 1, the probability mass in Figure 7 is most heavily weighted away from the distribution's center, indicating that the particle is more likely to be found far away from where it started than it is to be found close to where it started. This may be the biggest qualitative difference between the distributions of classical and quantum random walks: quantum walks tend to spread out, while classical random walks tend to hover around where they started.

2.2 Modifying the initial state to get a symmetric distribution

The fact that Figures 7a and 7b are mirror images of each other may make it seem like we should expect to get a symmetric distribution if we use the initial state

$$|\Psi_0\rangle = \frac{1}{\sqrt{2}} \left(|\uparrow \ 0\rangle + |\downarrow \ 0\rangle \right) \tag{76}$$

However, this is not the case. Figure 8, shows the distribution after 100 steps of a quantum walk with the initial state given by (76).

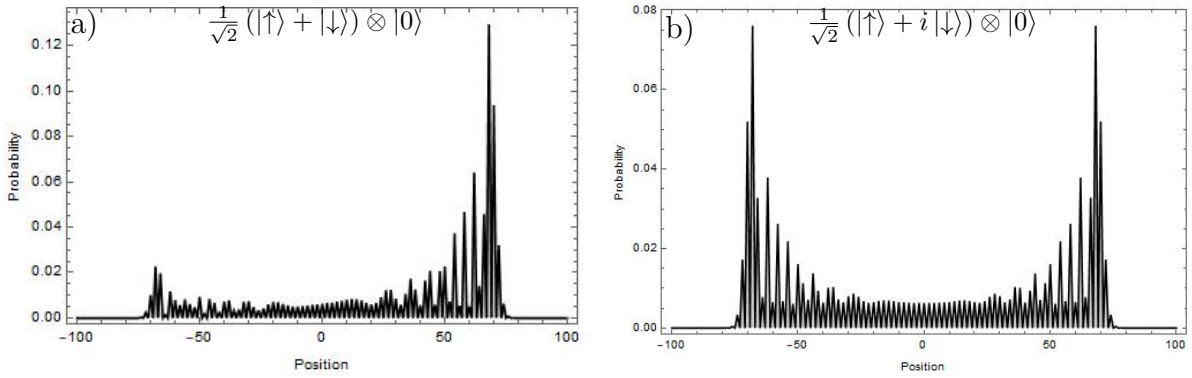

Figure 8: Both figures show the distribution for after 100 steps of a Hadamard on a line. 8a was simulated using initial state $|\Psi_0\rangle = \frac{1}{\sqrt{2}}(|\uparrow\ 0\rangle + |\downarrow\ 0\rangle)$. This distribution looks very similar to Figure 7a, but careful comparison of the two distributions around $x = 50$ shows that they are not quite the same. 8b used initial state $|\Psi_0\rangle = \frac{1}{\sqrt{2}}(|\uparrow\ 0\rangle + i\,|\downarrow\ 0\rangle)$, which resulted in a symmetric probability distribution.

Figure 8a shows a distribution that looks a lot like the distribution for the 100-step Hadamard walk with initial state $|\uparrow\ 0\rangle$, that is shown in Figure 7a. However, the two distributions are not quite the same. This can be seen computationally from the fact that the two distributions have different values for $\langle x\rangle$ and σ^2, which can be compared in Table 1. This difference can also be seen visually, through careful comparison of Figure 8 with Figure 7a around $x = 50$ (Figure 8 has two very closely spaced spikes around $x = 50$ and Figure 7a does not).

If we instead, define the initial state as

$$|\Psi_0\rangle = \frac{1}{2}(|\uparrow\ 0\rangle + i\,|\downarrow\ 0\rangle) \tag{77}$$

we get the symmetric distribution shown in Figure 8b. It's tempting to think that the distribution in Figure 8b might not quite be symmetric, since the expectation values and variances shown in Table 1 indicate that Figures 7a and 7b are not quite mirror reflections of each other. But if we calculate an expectation and variance for each half of the distribution in Figure 8b, by summing over $[-100, 0]$ in (74) for the left half of the distribution, and over $[0, 100]$ for the right half, we find that $\langle x_{left}\rangle = -25$ and $\langle x_{right}\rangle = 25$, and both halves have a variance of $\sigma^2 = 2304.42$, so it does appear to be exactly symmetric about $x = 0$, in spite of the fact that Figures 7a, 7 are not exactly mirror reflections of each other. An alternative approach to verifying this symmetry would be to go through and calculate the probability at each point and make sure that it is the same for each $\pm x$.

2.3 Modifying the coin operator to get a symmetric distribution

In the previous section we were able to produce a Hadamard walk with a symmetric distribution by using an initial state (77) whose eigenstates were 90° out of phase with each other.

Eigenstates in the two branches remained 90° out of phase with each other throughout the duration of the random walk, as a result of the fact that the Hadamard coin only enacts 180° phase changes. So two eigenstates that start off 90° out of phase will evolve as two branches that remain 90° out of phase throughout the duration of the Hadamard walk.

The end result is a symmetric distribution, which may be thought of as having been produced by superimposing two asymmetric distributions (specifically, the two distributions shown in Figure 7) that were 90° out of phase with each other.

An alternative approach to producing the symmetric distribution in Figure 8b is to start with the initial state that is in a spin-superposition of two states that are in-phase with one another

$$|\Psi_0\rangle = \frac{1}{\sqrt{2}}\left(|\uparrow\ 0\rangle + |\downarrow\ 0\rangle\right) \tag{78}$$

and let it time evolve under the action of a coin operator

$$C = \frac{1}{\sqrt{2}}\begin{pmatrix} 1 & i \\ i & 1 \end{pmatrix} \tag{79}$$

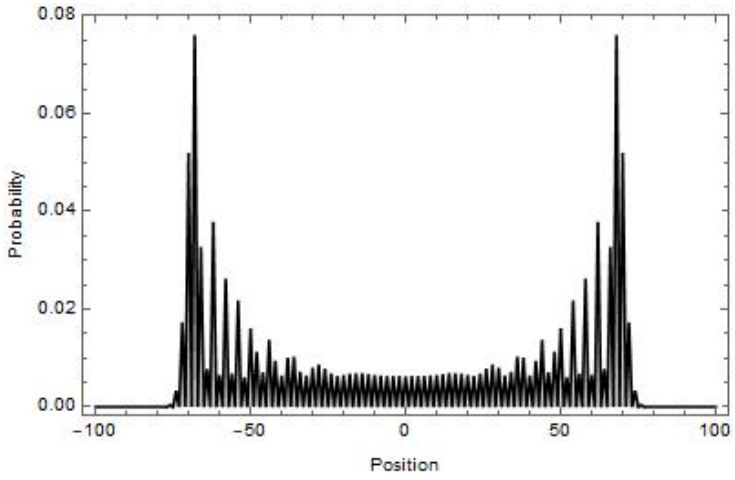

Figure 9: Symmetric probability distribution after 100 steps of a quantum random walk on a line with coin operator $\frac{1}{\sqrt{2}}\left(\begin{smallmatrix} 1 & i \\ i & 1 \end{smallmatrix}\right)$ and initial state $|\Psi_0\rangle = \frac{1}{\sqrt{2}}\left(|\uparrow\ 0\rangle + |\downarrow\ 0\rangle\right)$. This distribution is identical to Figure 8b, but was created using a different initial state and coin operator.

After 100 steps, the quantum walk's symmetric distribution, shown in Figure 9, has an expected position $\langle x\rangle = 0$ with variance $\sigma^2 = 2929.42$. Table 1 indicates that this is the same as for the Hadamard walk with initial state $\frac{1}{\sqrt{2}}\left(|\uparrow\ 0\rangle + |\downarrow\ 0\rangle\right)$, that is shown in Figure 8b.

2.4 Bounding the Quantum Walk with an Absorbing Boundary

An interesting case of quantum weirdness arises when we consider a quantum walk in the presence of an absorbing boundary [1, 11]. Placing an absorbing boundary at a position $|b\rangle$

can be viewed as equivalent to making a partial measurement on the particle's position at $|b\rangle$, at the end of every time step. This can be done by adding a position measurement operator M as the last operation in the suite of operations that comprise the evolution operator

$$U = (I \otimes M) \cdot S \cdot (H \otimes I) \tag{80}$$

where $M = M_b + M_{B_\perp}$ is the resolution of the identity into orthogonal projection operators that correspond to the $b, B_\perp$ eigenspaces.

We want to find the probability that the particle will have been absorbed by the absorbing boundary by the end of the N^{th} time step. To see the effect of applying M at the end of every time step, we need to first project the particle's wavefunction onto the basis $\{|b\rangle, |B_\perp\rangle\}$

$$\begin{aligned} |\Psi\rangle &= I\,|\Psi\rangle \\ &= (|b\rangle\langle b| + |B_\perp\rangle\langle B_\perp|)\,|\Psi\rangle \\ &= \langle b|\Psi\rangle\,|b\rangle + \langle B_\perp|\Psi\rangle\,|B_\perp\rangle \end{aligned} \tag{81}$$

Acting on both sides from the left with $\langle\Psi|$ gives

$$\begin{aligned} 1 &= \langle\Psi|\Psi\rangle \\ &= |\,\langle b|\Psi\rangle\,|^2 + |\,\langle B_\perp|\Psi\rangle\,|^2 \end{aligned} \tag{82}$$

which rearranges to

$$\langle B_\perp|\Psi\rangle = \sqrt{1 - |\,\langle b|\Psi\rangle\,|^2} \tag{83}$$

Rearranging (81) as an expression for $|B_\perp\rangle$, and then replacing $\langle B_\perp|\Psi\rangle$ in the denominator with (83) gives

$$|B_\perp\rangle = \frac{|\Psi\rangle - \langle b|\Psi\rangle\,|b\rangle}{\sqrt{1 - |\,\langle b|\Psi\rangle\,|^2}} \tag{84}$$

Substituting (83),(84) into (81) gives

$$|\Psi\rangle = \langle b|\Psi\rangle\,|b\rangle + \sqrt{1 - |\,\langle b|\Psi\rangle\,|^2}\left(\frac{|\Psi\rangle - \langle b|\Psi\rangle\,|b\rangle}{\sqrt{1 - |\,\langle b|\Psi\rangle\,|^2}}\right) \tag{85}$$

So a partial measurement $M = M_b + M_{B_\perp}$ on the particle's position gives

$$M\,|\Psi\rangle = \begin{cases} |b\rangle, & \text{with probability } |\,\langle b|\Psi\rangle\,|^2 \\ \dfrac{|\Psi\rangle - \langle b|\Psi\rangle\,|b\rangle}{\sqrt{1 - |\,\langle b|\Psi\rangle\,|^2}}, & \text{with probability } 1 - |\,\langle b|\Psi\rangle\,|^2 \end{cases} \tag{86}$$

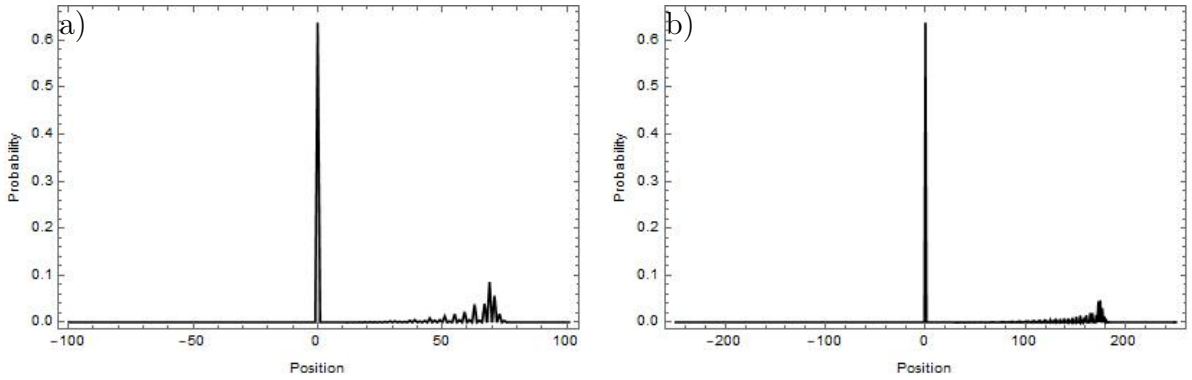

Figure 10: a,b are simulations after 100, 250 steps of a Hadamard walk in the presence of an absorbing boundary placed at $x = 0$. The simulation used initial state $|\Psi_0\rangle = |\uparrow\rangle \otimes |1\rangle$. Even after 2.5 times as many steps, the probability for the particle to have been absorbed in 10b is not discernibly any different from 10a. Quantum mechanics predicts a 36.34% probability that the particle will never be absorbed; in both cases the probability that the particle has been absorbed is about 0.6366. In contrast, there is a 100% probability for a classical particle to eventually be absorbed.

Figure 10 shows a quantum walk using the Hadamard coin, with the particle initially located at $x = 1$, and an absorbing boundary placed at $x = 0$. Measurements made during the simulation, on the probability for the particle to be absorbed by its $N^{th} = 1, 3, 10, 100, 250$ step are shown in Table 2.

steps	probability
1	0.5
3	0.625
10	0.63281
100	0.63658
250	0.63661

Table 2: Measured probabilities for the particle to be absorbed by the boundary at $x = 0$ during its first N steps of a Hadamard quantum walk on a line with initial state $|\Psi_0\rangle = |\uparrow\rangle \otimes |1\rangle$. These measurements, taken during runs of the simulation in Figure 10, appear to asymptote toward the limit $\frac{\pi}{2} \simeq 0.63662$ that was theorized in [11].

Classically, the probability of the particle being absorbed by the boundary at $x = 0$ approaches one as the number of steps becomes arbitrarily large. An easy way to see this is to consider the probability for a classical particle that makes it to $x = i$, to be at $x = 0$ in exactly i steps, and sum over the probabilities for all positions x the particle could reach before turning around.

On each step, the particle moves either left or right, with probability $\frac{1}{2}$. On its first step, at $x = 1$, the particle moves into the boundary at $x = 0$ or to $x = 2$, each with probability $\frac{1}{2}$. So we know that the total probability that the particle will eventually be absorbed is $\geq \frac{1}{2}$.

Now suppose that the particle makes it to $x = 2$, then there is a $\left(\frac{1}{2}\right)^2 = \frac{1}{4}$ probability that the particle will end up at $x = 0$ after two more steps. So we know that the total probability for the particle to eventually be absorbed is $\geq \frac{1}{2} + \frac{1}{4} = \frac{3}{4}$. Suppose the particle makes it to $x = 3$. Then there is a $\left(\frac{1}{2}\right)^3 = \frac{1}{8}$ probability that the particle will be at $x = 0$ immediately after taking its next three steps. So the total probability for the particle to be absorbed is $\geq \frac{1}{2} + \frac{1}{4} + \frac{1}{8}$. Continuing this line of reasoning for all positive integer values of x

$$\begin{aligned} Prob\left(\begin{smallmatrix}\text{classical particle}\\ \text{eventually hits}\\ \text{absorbing boundary}\end{smallmatrix}\right) &\geq \sum_{i=1}^{\infty} \frac{1}{2^i} \\ &= \left(\sum_{i=0}^{\infty} \frac{1}{2^i}\right) - 1 \\ &= \frac{1}{1-\frac{1}{2}} - 1 \\ &= 1 \end{aligned} \tag{87}$$

So classically there is a 100% probability that the particle will eventually be absorbed by the boundary at $x = 0$.

Surprisingly, quantum mechanics predicts that the same is not true for a quantum particle [11]. In the limit of an infinite number of steps of a Hadamard walk on a line, in the presence of an absorbing boundary at $x = 0$, and with initial state $|\uparrow\rangle \otimes |0\rangle$, the probability that the particle will eventually be absorbed is

$$\begin{aligned} Prob\left(\begin{smallmatrix}\text{quantum particle}\\ \text{eventually hits}\\ \text{absorbing boundary}\end{smallmatrix}\right) &= \frac{2}{\pi} \\ &\simeq 0.63662 \end{aligned} \tag{88}$$

(see Theorem 8 in the *Results for semi-infinite and finite Hadamard walks* section of [11]).

The results from the simulation in Figure 10 are shown in Table 2, and appear to asymptote toward this limit. So classically there is a 100% probability that the particle will eventually be absorbed, but quantum mechanics predicts that there is a 36.34% probability that the particle will never be absorbed.

The reason for this can be understood by comparing Figure 1, for a classical random walk on a line, to Figure 7a, for a Hadamard walk on a line. The classical particle in Figure 1 tends to stay close to its initial position, near $x = 0$, while the quantum particle in Figure 7a, shows the opposite tendency, of distancing itself from its initial position as the number of time steps increases.

2.5 Quantum Walk on a Circle

A quantum walk on a line can be turned into a quantum walk on a circle, or n-polygon, by imposing periodic boundary conditions on the line. This can be done by imposing the periodicity on the ket vector components of the position space dyads in (68)

$$|i\rangle \to |i \mod n\rangle \tag{89}$$

This gives us the conditional translation operator for a quantum walk on a circle with n positions available for the particle to occupy

$$S_{circle} = |\uparrow\rangle\langle\uparrow| \otimes \sum_{i=0}^{n-1} |i+1 \bmod n\rangle\langle i| + |\downarrow\rangle\langle\downarrow| \otimes \sum_{i=0}^{n-1} |i-1 \bmod n\rangle\langle i| \tag{90}$$

Still using the Hadamard coin, the time evolution operator for this quantum walk is

$$U = S_{circle} \cdot (H \otimes I) \tag{91}$$

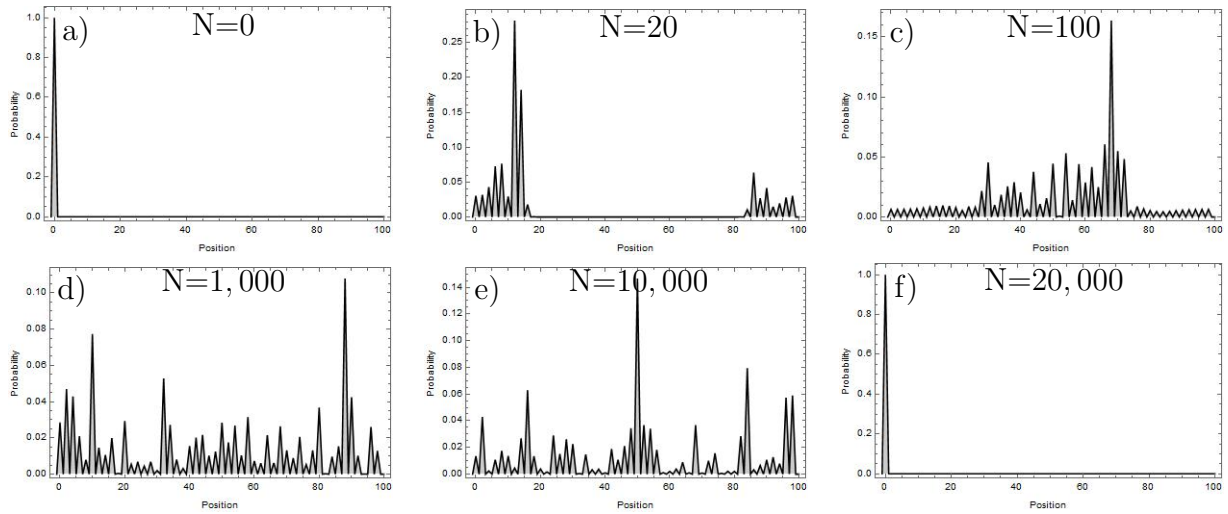

Figure 11: a,b,c,d,e show simulations after 0, 20, 100, 1,000, and 10,000 steps of a Hadamard walk on a circle that has 100 occupiable positions, and with $x = 0$ being identified with $x = 100$. Each simulation used initial state $|\uparrow\ 0\rangle$. 11f shows the simulation after another 10,000 steps, except with the time evolution operator U being replaced by its hermitian conjugate $U^\dagger$, as it is defined in (100). These additional 10,000 steps demonstrate that information about the initial state of the system was conserved, even after 10,000 steps.

Simulations for a Hadamard walk on a circle with 100 spatial positions are shown in Figure 11. After the first 100 steps, the wavefunction still has a reasonably definite position on one side of the circle. In contrast, Figure 11d shows that after 1,000 steps, the particle is much more evenly distributed around the circle. Figure 11e shows that the wavefunction seems to remain reasonably evenly distributed once it has spread out over the circle. 11f was reached after acting on $|\Psi_{10,000}\rangle$ 10,000 times with the time evolution operator's hermitian conjugate, to return the wavefunction to its initial state. Figure 11f demonstrates the fact that the information needed to reproduce the system's initial state is maintained in the wavefunction throughout the duration of the quantum walk, and is the topic of the upcoming section.

2.6 Conservation of information during a quantum walk

Unitary time evolution in quantum mechanics gives rise to the principle of conservation of information, which is the concept that if we have an equation $|\Psi\rangle$ that describes the time evolution of a quantum system, then we can always rewind our equation backward to a chosen time $t = 0$, when the system was in a state $|\Psi_0\rangle$, which is related to the system's present state $|\Psi(t)\rangle$ by

$$|\Psi(t)\rangle = U(t)\,|\Psi_0\rangle \tag{92}$$

This rewinding is done by acting on $|\Psi(t)\rangle$ with the evolution operator's hermitian conjugate $U^\dagger = U^{-1}$

$$|\Psi_0\rangle = U^\dagger(t)\,|\Psi(t)\rangle \tag{93}$$

So far we have been working with discrete time, so it makes sense to write the evolution operator as a function of the number of time steps $U = U(N)$ and treat it as an infinitesimal generator

$$U^{-1}(N) = \left[U^{-1}(0)\right]^N \tag{94}$$

To construct an inverse evolution operator, first note that the Hadamard operator (66) is self-inverse $H^{-1} = H$, which using the identity $(A \otimes B)^{-1} = A^{-1} \otimes B^{-1}$, gives the inverse Hadamard coin operator

$$(H \otimes I)^{-1} = H \otimes I \tag{95}$$

The conditional translation operator, as it was defined in (68), has an inverse S^{-1} that can be found by defining the inverse operator's action to do the opposite of what S was defined to do in (68), which is done with the replacement

$$|i \pm 1\rangle \to |i \mp 1\rangle \tag{96}$$

Making this replacement in (68) gives the inverse conditional translation operator

$$S^{-1} = |\uparrow\rangle\langle\uparrow| \otimes \sum_{i=-\infty}^{\infty} |i-1\rangle\langle i| + |\downarrow\rangle\langle\downarrow| \otimes \sum_{i=-\infty}^{\infty} |i+1\rangle\langle i| \tag{97}$$

Then applying the matrix identity $(A \cdot B)^{-1} = B^{-1} \cdot A^{-1}$ to (69), we have the inverse time evolution operator

$$U^{-1} = (H \otimes I) \cdot S^{-1} \tag{98}$$

Using computational software it can be shown that even after 100 steps of a Hadamard walk on a line, we are still able to rewind the particle backward through its quantum walk, all the way back to its initial state[4]

[4] As mentioned before, $|\Psi_{100}\rangle$ in (99) only contains kets with even x-values because during a Hadamard walk, the particle can only be at positions that have the same even-or-odd parity the number of time steps N that it has taken. This property is true for both classical and (Hadamard) quantum random walks.

$$
\begin{aligned}
\left(U^{-1}\right)^{100}|\Psi_{100}\rangle = \left(U^{-1}\right)^{100}\Bigg[& |\uparrow\rangle \otimes \Bigg(\frac{1}{1125899906842624}|-98\rangle + \frac{95}{1125899906842624}|-96\rangle \\
& + \frac{4275}{1125899906842624}|-94\rangle + ... + \frac{99}{1125899906842624}|98\rangle \\
& + \frac{1}{1125899906842624}|100\rangle \Bigg) \\
& + |\downarrow\rangle \otimes \Bigg(\frac{1}{1125899906842624}|-100\rangle + \frac{97}{1125899906842624}|-98\rangle \\
& + ... + \frac{4655}{1125899906842624}|96\rangle + \frac{1}{1125899906842624}|98\rangle \Bigg)\Bigg] \\
= & |\uparrow\rangle \otimes |0\rangle \\
= & |\Psi_0\rangle \qquad (99)
\end{aligned}
$$

This means that the information needed to regenerate the system's initial state was contained in the wavefunction throughout the entire duration of the quantum walk. The information about the wavefunction's initial state was conserved. In Section 2.6.2 we will show that this property seems to be the deciding factor as to whether or not a random walk behaves classically or quantumly.

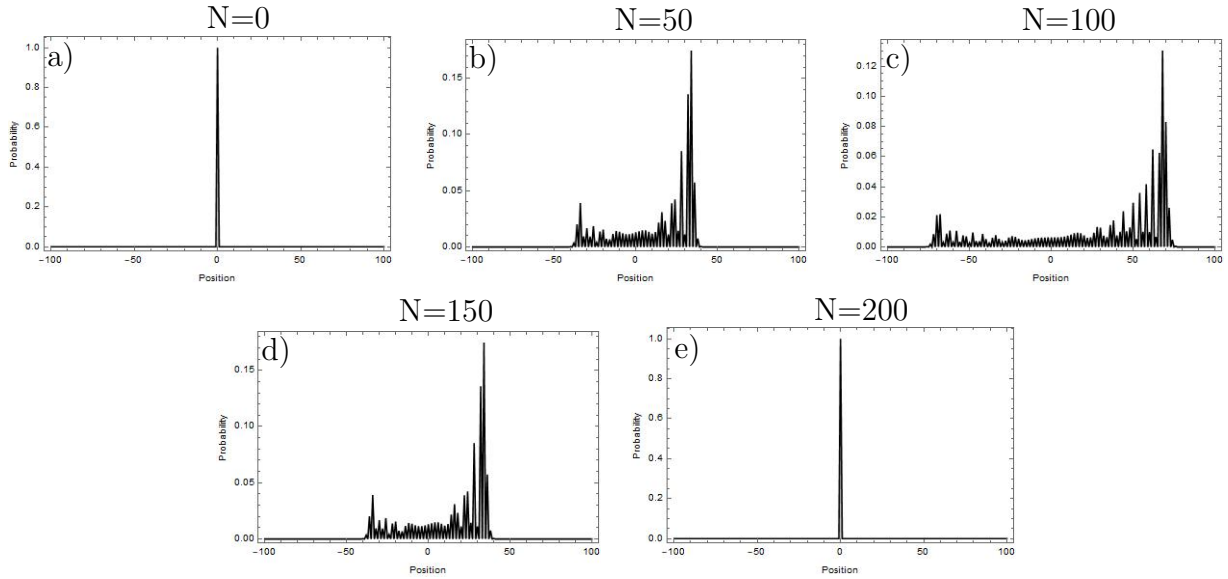

Figure 12: Simulations of a quantum walk on a line with the Hadamard operator and initial state $|\uparrow\rangle \otimes |0\rangle$. The first 100 steps evolv the system forward through time, to Figure 12*c*. The second 100 steps evolve the system with U replaced by $U^\dagger$, effectively time-evolving the wavefunction backwards through time, to its initial state. This simulation demonstrates that the information about the state of the system at $t = 0$ was conserved throughout the duration of the quantum walk. Classical random walks do not have this property because the classical random walk's analog of the quantum walk's S matrix is not invertible.

The same reversibility is true for a quantum walk on a circle, with the inverse evolution operator defined as

$$U_{circle}^{-1} = (H \otimes I) \cdot S_{circle}^{-1} \tag{100}$$

S_{circle}^{-1} is found the same way as S^{-1} in (97), by replacing $|i \pm 1 \mod n\rangle \to |i \mp 1 \mod n\rangle$ in (90). As was the case for after 100 steps of a Hadamard walk on a line, it can be shown using computational software that

$$\begin{aligned} |\Psi_{20,000}\rangle &= \left(U_{circle}^{-1}\right)^{10,000} |\Psi_{10,000}\rangle \\ &= |\uparrow\rangle \otimes |0\rangle \\ &= |\Psi_0\rangle \end{aligned} \tag{101}$$

which was the initial state of the quantum walk in Section 2.5. However, after the quantum walk's first $10,000$ steps, the numerator of its first eigenstate $|\uparrow\rangle \otimes |0\rangle$, by itself, is 1505 characters long. So I've had to write (101) much more compactly than (99). A simulation of the return from $|\Psi_{10,000}\rangle$ to the wavefunction's initial state $|\Psi_{20,000}\rangle = |\Psi_0\rangle$ is shown in Figure 11f. This reversibility of quantum random walks is not a property of classical random walks, which is the topic of the upcoming section.

2.6.1 Comparison to irreversibility of a classical random walk

The irreversibility of a classical random walk can be demonstrated by expressing the probability distribution as a sequence of probability distributions indexed by time step n

$$P_{n+1} = MP_n \tag{102}$$

and then show that this sequence is irreversible as a result of the matrix M not being invertible. Reversibility would mean there exists an inverse matrix $M-1$ such that

$$P_n = M^{-1}P_{n+1} \tag{103}$$

For a classical random walk on an infinite line we would need for M to be infinite-dimensional. To avoid this problem, we can consider a classical random walk on the vertices of a square, labeled as x_0, x_1, x_2, x_3

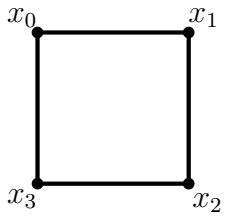

We can represent these positions by a set of mutually orthogonal column vectors

$$x_0 = \begin{pmatrix} 1 \\ 0 \\ 0 \\ 0 \end{pmatrix}, \quad x_1 = \begin{pmatrix} 0 \\ 1 \\ 0 \\ 0 \end{pmatrix}, \quad x_2 = \begin{pmatrix} 0 \\ 0 \\ 1 \\ 0 \end{pmatrix}, \quad x_3 = \begin{pmatrix} 0 \\ 0 \\ 0 \\ 1 \end{pmatrix} \tag{104}$$

For simplicity we can consider the special case of an unbiased random walk. During any given time step, the particle either moves clockwise or counterclockwise, each with probability $\frac{1}{2}$. From this we are able to define a matrix M of transition probabilities for this particle, by considering the action of M on the particle's position states

$$\begin{pmatrix} 1 \\ 0 \\ 0 \\ 0 \end{pmatrix} \to \begin{pmatrix} 0 \\ 1/2 \\ 0 \\ 1/2 \end{pmatrix}, \qquad \begin{pmatrix} 0 \\ 1 \\ 0 \\ 0 \end{pmatrix} \to \begin{pmatrix} 1/2 \\ 0 \\ 1/2 \\ 0 \end{pmatrix}, \qquad \begin{pmatrix} 0 \\ 0 \\ 1 \\ 0 \end{pmatrix} \to \begin{pmatrix} 0 \\ 1/2 \\ 0 \\ 1/2 \end{pmatrix}, \qquad \begin{pmatrix} 0 \\ 0 \\ 0 \\ 1 \end{pmatrix} \to \begin{pmatrix} 1/2 \\ 0 \\ 1/2 \\ 0 \end{pmatrix} \tag{105}$$

$$M = \begin{pmatrix} 0 & 1/2 & 0 & 1/2 \\ 1/2 & 0 & 1/2 & 0 \\ 0 & 1/2 & 0 & 1/2 \\ 1/2 & 0 & 1/2 & 0 \end{pmatrix} \tag{106}$$

We need to find an inverse matrix M^{-1} to be able to use (103) to rewind the random walk backward to its previous states. However

$$\det M = 0 \tag{107}$$

which means that M is not invertible. So whenever M propagates the classical particle forward through one time step, we lose the information needed to be able to reconstruct the particle's previous state. As we show in the next section, it is this loss of reversibility that is needed in order for a quantum walk to behave classically.

2.6.2 Producing a classical distribution with a quantum walk

Consider a particle in the initial state

$$|\Psi_0\rangle = \frac{1}{\sqrt{2}} \left(|\uparrow\rangle + |\downarrow\rangle \right) \otimes |0\rangle \tag{108}$$

In this random walk, during each time step, the particle is first acted on by the conditional translation operator S defined by (68). After the translation we assume that a measurement is made on the particle, so that it is forced to choose a state of definite spin. The step ends with a reinitialization of each eigenstate to a spin-superposition

$$|\uparrow\rangle \otimes |0\rangle \to \frac{1}{\sqrt{2}} \left(|\uparrow\rangle + |\downarrow\rangle \right) \otimes |0\rangle \tag{109a}$$

$$|\downarrow\rangle \otimes |0\rangle \to \frac{1}{\sqrt{2}} \left(|\uparrow\rangle + |\downarrow\rangle \right) \otimes |0\rangle \tag{109b}$$

which corresponds to the matrix operator

$$R(N) = a(N) \begin{pmatrix} 1 & 1 \\ 1 & 1 \end{pmatrix} \tag{110}$$

acting on the particle's coin space $\mathcal{H}_C$. $a(N)$ is a normalization constant that is a function of the number of time-steps, which must be applied at the end to account for the fact that $R(N)$ is nonunitary

$$\det R = 0 \tag{111}$$

The nonunitarity of R can be viewed as being a result of the measurment-like process that causes the quantum particle to decohere from its spin-superposition, into a state of definite spin.

The evolution operator for this process is

$$(R \otimes I) \cdot S \tag{112}$$

which I am not labeling as U, out of emphasize for the fact that it is not unitary.

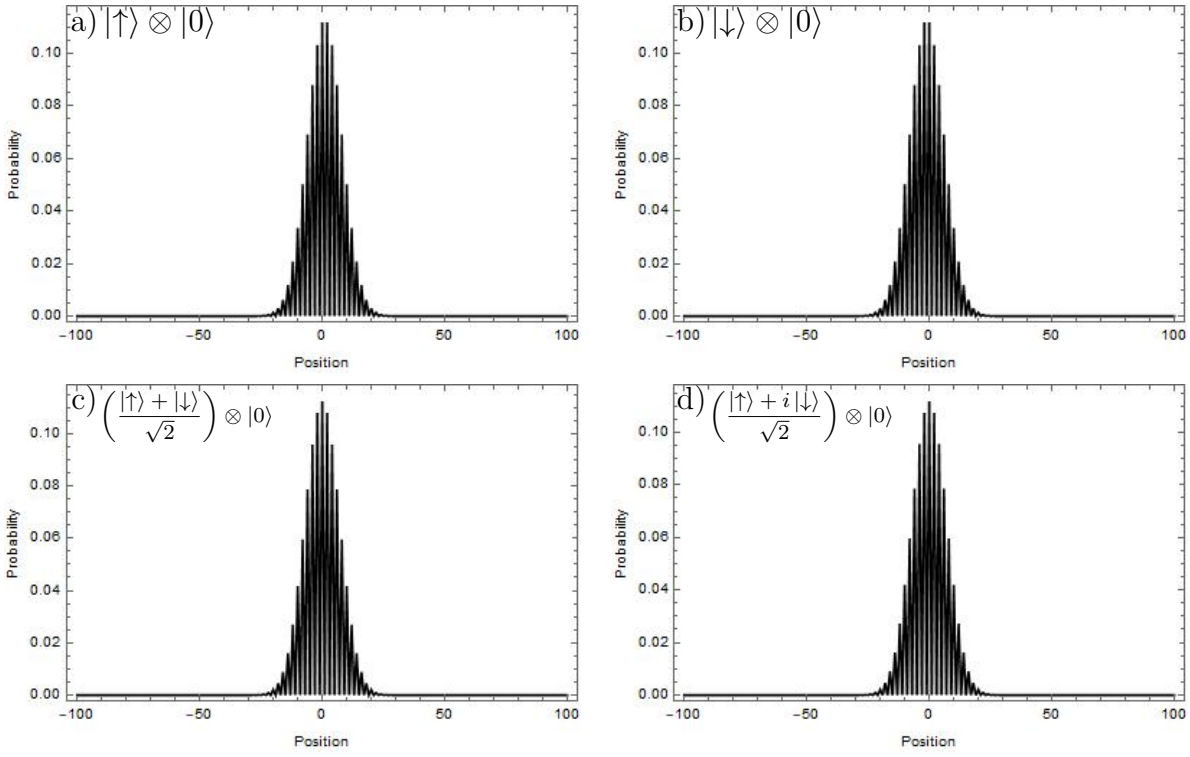

Figure 13: The distributions for four different initial states, after 100 steps of the random walk that is generated by the operator defined in (112). *Nonunitarity* of the evolution operator for this random walk gives rise to a distribution that resembles the distribution of a classical random walk. The shape of the distribution has a surprisingly weak dependence on the particle's initial state. $\langle x \rangle$ and σ^2 for each distribution is given in Table 3.

Figure 13 shows that the distributions for each figure's indicated initial state, after 100 steps of the random walk enacted by (112). Table 3 shows the particle's expected position and variance for each random walk. For all four simulations, the expected position of the

particle is either $\langle x \rangle = 0$ or within one step of it, and the variance is about $\sigma^2 = 50$ for each simulation. This is smaller than the variance of the classical random walk shown in Figure 3, which has a variance $\sigma^2 = 100$, but is still much more comparable to the variance of a classical random walk than to the variances of the Hadamard walks shown in Table 1.

$\|\Psi_0\rangle$	$\langle x \rangle$	σ^2
$\|\uparrow\rangle \otimes \|0\rangle$	1	49.7513
$\|\downarrow\rangle \otimes \|0\rangle$	-1	49.7513
$\frac{1}{\sqrt{2}}(\|\uparrow\rangle + \|\downarrow\rangle) \otimes \|0\rangle$	0	50.2513
$\frac{1}{\sqrt{2}}(\|\uparrow\rangle + i\|\downarrow\rangle) \otimes \|0\rangle$	0	50.7513

Table 3: Expectation and variance of the particle's position after 100 steps of a random walk using the evolution operator defined in (112).

Another approach to producing a classical distribution with a quantum walk is discussed in [13]. Their approach was done in 2-dimensions, and used a generalized version of the Hadamard coin operator

$$H(\beta) = \begin{pmatrix} 1 & e^{i\beta} \\ e^{-i\beta} & -1 \end{pmatrix} \tag{113}$$

which becomes exactly Hadamard for the special case $\beta = 0$. At the beginning of each time step, they randomly chose a value for $\beta \in [0, 2\pi)$, which added randomness the wavefunction's time evolution. Their model produced a very classical-looking distribution, using only unitary operations. However, it does appear to have some probability mass that escaped the central distribution, and made it out to around $(x, y) = (0, -100)$ and $(-100, 0)$, where as the distributions shown in Figure 13 have all of their probability mass centrally-located, which is more consistent with the actual distribution for a classical random walk. Furthermore, it is more classical for the system to time evolve in a way that is nonunitary, as indicated by (107) and (111).

2.7 Quantum Walks in Two Dimensions

The Hadamard walk on a line can be extended to higher dimensions by finding any higher-dimensional operator that reduces to (66) for the special case of a random walk in one spatial dimension. Two such generalizations considered here are $H^{\otimes n}$ and the n-dimensional discrete Fourier transform DFT_n. The simulations given here are replications of the work done in [13].

2.7.1 Generalization to $H^{\otimes n}$

A quantum walk in n spatial dimensions requires a $2n$-dimensional coin space to keep track of the particle's probability distribution in space. We an define the coin space $\mathcal{H}_C^{\otimes n}$

as a tensor product of coin spaces for n qubits. We can then think of each qubit as being assigned to keep track of the distribution's time-evolution along one spatial dimension. With this approach, we can define the particle's position space $\mathcal{H}_P^{\otimes n}$ as a tensor product of the 1-dimensional position spaces that the qubits are assigned to keep track of. So our Hilbert space is then defined as $\mathcal{H} = \mathcal{H}_C^{\otimes n} \otimes \mathcal{H}_P^{\otimes n}$.

The simulations presented in this section take place in two spatial dimensions, so we can define our Hilbert space as $\mathcal{H} = \mathcal{H}_C^{\otimes 2} \otimes \mathcal{H}_P^{\otimes 2}$, with basis vectors $|m_{s_1}\ m_{s_2}\ x\ y\rangle$.

The 2-dimensional conditional translation operator can be defined as

$$S_2 = \sum_{i=-\infty}^{\infty} \sum_{j=-\infty}^{\infty} \Big\{ |\uparrow\ \uparrow\rangle\langle\uparrow\ \uparrow| \otimes |i{+}1\ j{+}1\rangle\langle i\ j| + |\uparrow\ \downarrow\rangle\langle\uparrow\ \downarrow| \otimes |i{+}1\ j{-}1\rangle\langle i\ j| \\ + |\downarrow\ \uparrow\rangle\langle\downarrow\ \uparrow| \otimes |i{-}1\ j{+}1\rangle\langle i\ j| + |\downarrow\ \downarrow\rangle\langle\downarrow\ \downarrow| \otimes |i{-}1\ j{-}1\rangle\langle i\ j| \Big\} \quad (114)$$

To define the system's time evolution, it is enough to specify the evolution operator's action on each of the basis vectors of our Hilbert space

$$\begin{aligned} |\uparrow\ \uparrow\ x\ y\rangle &\to |\uparrow\ \uparrow\ (x{+}1)\ (y{+}1)\rangle \\ |\uparrow\ \downarrow\ x\ y\rangle &\to |\uparrow\ \downarrow\ (x{+}1)\ (y{-}1)\rangle \\ |\downarrow\ \uparrow\ x\ y\rangle &\to |\downarrow\ \uparrow\ (x{-}1)\ (y{+}1)\rangle \\ |\downarrow\ \downarrow\ x\ y\rangle &\to |\downarrow\ \downarrow\ (x{-}1)\ (y{-}1)\rangle \end{aligned} \quad (115)$$

Simulations after 10 steps of this quantum walk, for different initial states, are shown in Figure 14.

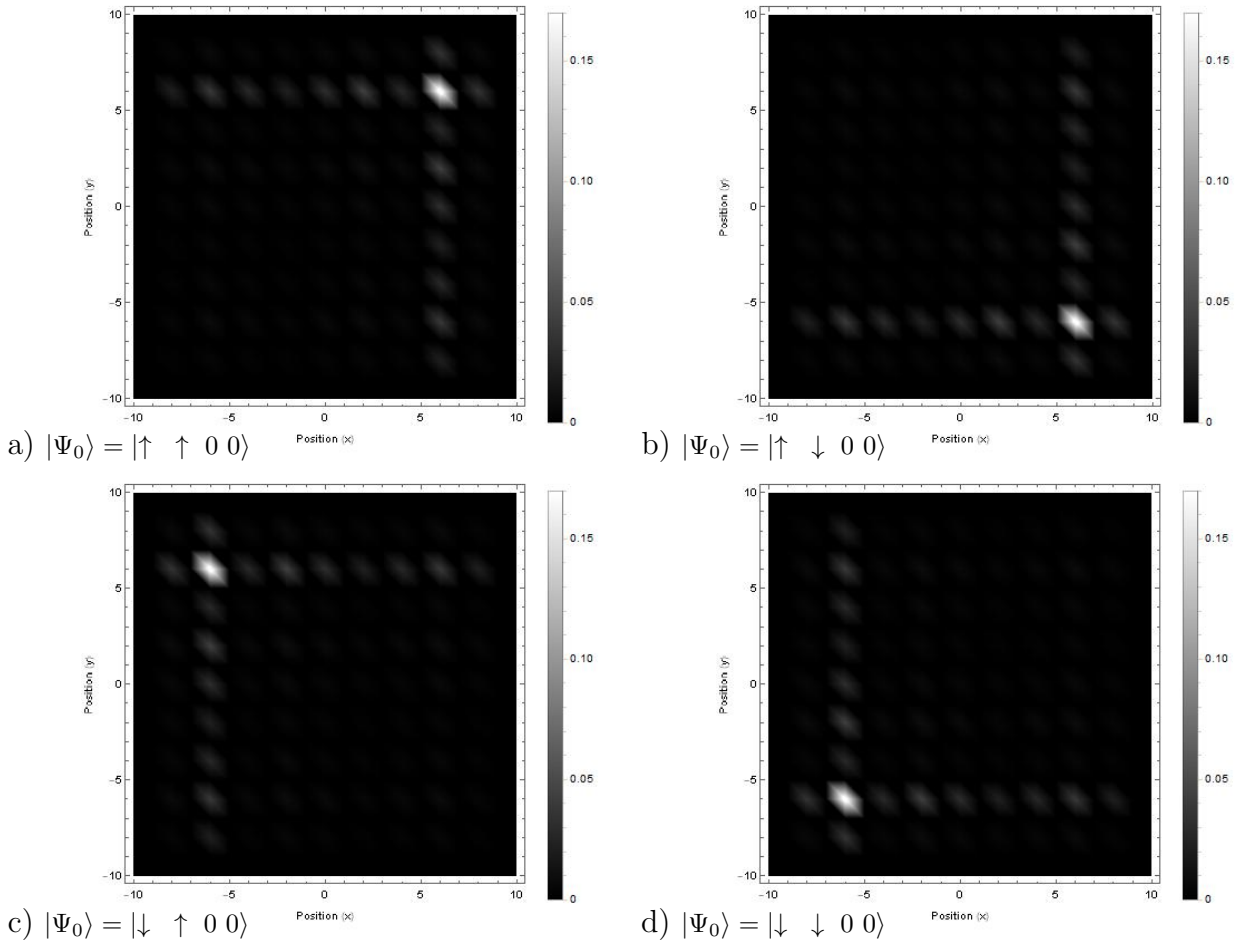

Figure 14: a,b,c,d show quantum mechanical predictions for the probability density plots for simulations of a 2-dimensional quantum walk, using different initial states. Each simulation used 10 iterations and coin flip operator $H^{\otimes 2}$. The spin configuration of each initial state gives rise to different reflections of the same distribution shape.

Figure 14 shows the 2-dimensional quantum walk simulations that were done using $H^{\otimes 2}$ as the coin operator. Each initial state was a single eigenstate with a different spin configuration. These simulations show that changing the wavefunction's initial spin-state has the effect or reflecting the overall distribution over the x- and y-axes.

Just as for a random walk in one dimension (both classical and Hadamard quantum walks), a quantum walk in two dimensions has nonzero probability only for spatial positions that have the same even-or-odd parity as the total number of time steps taken (this is also true of a classical random walk in two dimensions, and is visible in Figure 5). So the dark fringes seen between the bright fringes in each simulation are a result of the fact that there is zero probability of the particle landing on odd values of x and y, since the simulations show the distribution immediately after the particle's 10^{th} time step, which is an even number of steps.

C	$\|\Psi_0\rangle$	$\langle x\rangle$	$\langle y\rangle$	σ_x^2	σ_y^2
$H^{\otimes 2}$	$\|\uparrow\ \uparrow\rangle \otimes \|0\ 0\rangle$	2.4531	2.4531	23.9354	23.9354
$H^{\otimes 2}$	$\|\uparrow\ \downarrow\rangle \otimes \|0\ 0\rangle$	2.4531	−2.4531	23.9354	23.9354
$H^{\otimes 2}$	$\|\downarrow\ \uparrow\rangle \otimes \|0\ 0\rangle$	−2.4531	2.4531	23.9354	23.9354
$H^{\otimes 2}$	$\|\downarrow\ \downarrow\rangle \otimes \|0\ 0\rangle$	−2.4531	−2.4531	23.9354	23.9354
DFT_2	$\|\downarrow\ \downarrow\rangle \otimes \|0\ 0\rangle$	−1.6	−1.4966	19.0518	18.1372

Table 4: Initial state $|\downarrow\ \downarrow\ 0\ 0\rangle$Expectation and variance of the particle's position after 100 steps of the Hadamard walk simulations done in this section.

The expectation values and and variances of the particle's position for the distributions shown in Figure 14 are provided in Table 5. As you might guess from looking at Figure 14, the expectation's magnitude and the variance are of the same for all four simulations, along both axes $|\langle x\rangle| = |\langle y\rangle| = 2.4531$, $\sigma_x^2 = \sigma_y^2 = 23.9354$. This symmetry between the x- and y-directions is a result of the fact that $H^{\otimes n}$ does not produce entanglement between the spin-states corresponding to different spatial dimensions. As we will see in the next section, this symmetry breaks down when we run the same simulation with $H^{\otimes 2}$ replaced by DFT_2, which does produce entanglement.

2.7.2 Generalization to DFT_n

Another option for generalizing the Hadamard coin to higher dimensions is the 2^n-dimensional discrete Fourier transform DFT_n, which unlike $H^{\otimes n}$, does produce entanglement between the spin-states of different spatial dimensions. Just like $H^{\otimes n}$, DFT_n acts on the coin space $\mathcal{H}_C^{\otimes n}$, that is a tensor product of single-qubit coin spaces, and is defined as

$$DFT_n |j\rangle = \frac{1}{\sqrt{2}} \sum_{k=0}^{n-1} \omega^{jk} |k\rangle \tag{116}$$

where $\omega^{jk} = e^{i2\pi jk/2^n}$, and $|j\rangle, |k\rangle$ are basis vectors of the n-qubit coin space ${\mathcal{H}_\mathcal{C}}^{\otimes n}$, which is a $2n$-dimensional Hilbert space.

To show that (116) reduces to the Hadamard coin for the case of one spatial dimension, we need to make a change of notation, letting $|\uparrow\rangle, |\downarrow\rangle$ correspond to $|0\rangle, |1\rangle$, respectively. The action of DFT_1 on the basis states $|0\rangle, |1\rangle$ of our 2-dimensional coin space $\mathcal{H}_\mathcal{C}$

$$DFT_1 |0\rangle = \frac{1}{\sqrt{2}} (|0\rangle + |1\rangle) \tag{117a}$$

$$DFT_1 |1\rangle = \frac{1}{\sqrt{2}} (|0\rangle - |1\rangle) \tag{117b}$$

which has the matrix representation

$$DFT_1 = \frac{1}{\sqrt{2}} \begin{pmatrix} 1 & 1 \\ 1 & -1 \end{pmatrix} \tag{118}$$

and is the Hadamard coin from (66). This proves that DFT_n is a higher-dimensional generalization of the Hadamard coin.

To simulate a 2-dimensional quantum walk with DFT_2 we need to determine the action of DFT_2 on the basis states of our now 4-dimensional coin space ${\mathcal{H}_C}^{\otimes 2}$. Once again, to find out how the basis vectors transform, we need to first make a change of notation, letting $|\uparrow\uparrow\rangle, |\uparrow\downarrow\rangle, |\downarrow\uparrow\rangle, |\downarrow\downarrow\rangle$ correspond to $|0\rangle, |1\rangle, |2\rangle, |3\rangle$, respectively. Acting on the basis vectors of our coin space with DFT_2 gives

$$DFT_2 |0\rangle = \frac{1}{2}(|0\rangle + |1\rangle + |2\rangle + |3\rangle) \tag{119a}$$

$$DFT_2 |1\rangle = \frac{1}{2}(|0\rangle + i|1\rangle - |2\rangle - i|3\rangle) \tag{119b}$$

$$DFT_2 |2\rangle = \frac{1}{2}(|0\rangle - |1\rangle + |2\rangle - |3\rangle) \tag{119c}$$

$$DFT_2 |3\rangle = \frac{1}{2}(|0\rangle - i|1\rangle - |2\rangle + i|3\rangle) \tag{119d}$$

Replacing $|0\rangle, |1\rangle, |2\rangle, |3\rangle$ with $|\uparrow\uparrow\rangle, |\uparrow\downarrow\rangle, |\downarrow\uparrow\rangle, |\downarrow\downarrow\rangle$ in the above equation, and grabbing the conditional translation operator from (114), the evolution operator for this quantum walk is

$$U = S_2 \cdot (DFT_2 \otimes I_4) \tag{120}$$

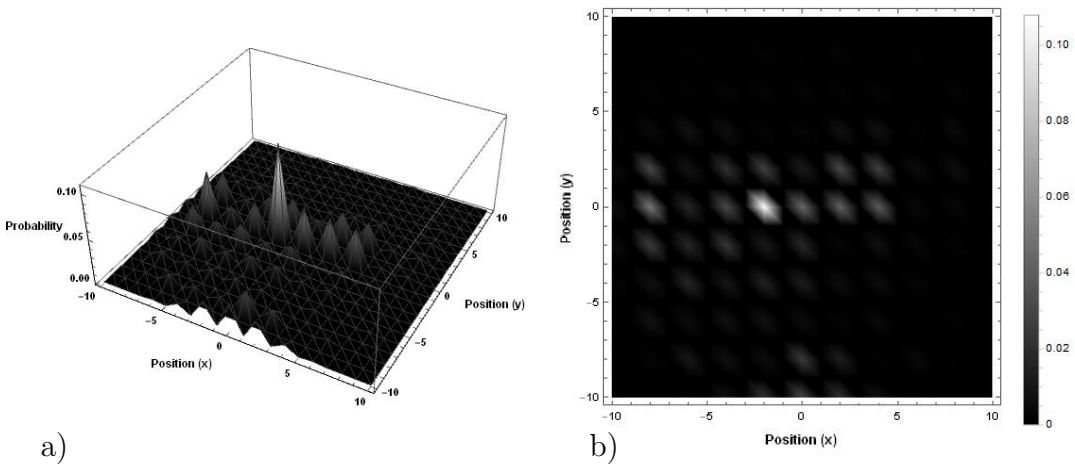

Figure 15: a,b show the probability distribution after 10 steps of a quantum walk in two spatial dimensions using the DFT_2 coin flip operator and initial state $|\downarrow \ \downarrow\rangle \otimes |0\ 0\rangle$.

C	$\langle x \rangle$	$\langle y \rangle$	σ_x^2	σ_y^2
$H^{\otimes 2}$	-2.4531	-2.4531	23.9354	23.9354
DFT_2	-1.6	-1.4966	19.0518	18.1372

Table 5: Comparison of the expectation value and variance of the particle's position after 10 steps of quantum walks with $H^{\otimes 2}$ and DFT_2 coin operators. Both quantum walks were simulated using the initial state $|\downarrow \ \downarrow\rangle \otimes |0\ 0\rangle$, for comparison with [13].

The interference pattern predicted by quantum mechanics is shown in Figure 15, and is consistent with the findings shown in Figure 4 of [13]. Their simulation uses the same initial state $|\downarrow \ \downarrow \ 0 \ 0\rangle$ and coin operator DFT_2, but differs in that it uses over 100 iterations and was done on a 100×100 element lattice. Their distribution has the same shape as the one shown in Figure 15, except reflected about a diagonal line running from the bottom right hand side to the top left hand side of Figure 15b.

According to [11 ??], standard deviation of this n-dimensional generalization of the Hadamard walk is $\sigma_n = \sqrt{(n+1)/2})\Delta\sigma_1$, which means that the standard deviation increases with increasing number of spatial dimensions, at a lesser rate for quantum walks with a DFT_n coin operator than with a $H^{\otimes n}$ coin operator. This is consistent with the fact that the probability mass in Figure 15 is somewhat localized around the origin, in comparison to the distribution shown in Figure 14, where it spreads out over the grid's perimeter.

One thing that stands in Figure 15, which is in contrast to Figure 14, is the probability distribution's lack of symmetry between the two spatial dimensions. This is a result of the fact that DFT_2 produces entanglement between the spin-states of the two spatial dimensions, while $H^{\otimes 2}$ does not.

2.8 Quantum walk on a torus

An n-dimensional infinite Hadamard walk with coin operator $H^{\otimes n}$ can be turned into a Hadamard walk on an n-torus by imposing periodic boundary conditions on each dimension. The action of the evolution operator U on the basis states of our Hilbert space is

$$\begin{aligned}
|\uparrow \ \uparrow \ x \ y\rangle &\to |\uparrow \ \uparrow \ (x+1 \mod n) \ (y+1 \mod n)\rangle \\
|\uparrow \ \downarrow \ x \ y\rangle &\to |\uparrow \ \downarrow \ (x+1 \mod n) \ (y-1 \mod n)\rangle \\
|\downarrow \ \uparrow \ x \ y\rangle &\to |\downarrow \ \uparrow \ (x-1 \mod n) \ (y+1 \mod n)\rangle \\
|\downarrow \ \downarrow \ x \ y\rangle &\to |\downarrow \ \downarrow \ (x-1 \mod n) \ (y-1 \mod n)\rangle
\end{aligned} \tag{121}$$

which can be used to simulate the quantum walk

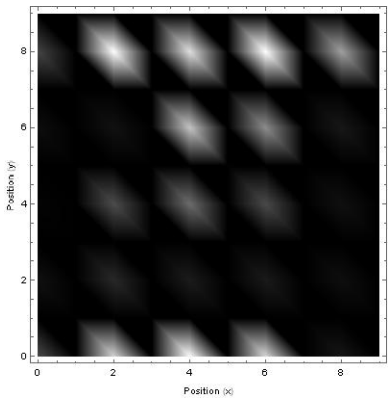

Figure 16: Simulation of a quantum walk after 10 steps, on a torus, with the particle having 10 accessible spatial positions along each of the two dimensions. This simulation used the $H^{\otimes 2}$ coin operator and initial state $|\Psi_0\rangle = |\uparrow \ \uparrow\rangle \otimes |0\ 0\rangle$.

The space in Figure 16 is a topological torus. In spite of its use of $H^{\otimes 2}$ as a coin operator, this quantum walk does not appear to have any noticeable symmetry. This is in contrast to the quantum walk shown in Figure 14a, which uses the same initial state and coin operator, and is symmetric about a diagonal line running from the bottom left corner to the top right corner of the distribution.

2.9 Weird predictions by a quantum random walk on a line

The following is based on [1, 14]. Consider a spin-$\frac{1}{2}$ particle whose wavefunction is located at position x_0, in the initial state

$$|\Psi\rangle = (a_\uparrow |\uparrow\rangle + a_\downarrow |\downarrow\rangle) \otimes |x_0\rangle \tag{122}$$

For this example, instead of working with the bulky conditional translation operator that was defined in (68), we will define a more simple conditional translation operator. Starting with a spatial translation operator $T(l)$, whose action is to shift the particle one unit of distance l to the right

$$|x\rangle \to |x + l\rangle \tag{123}$$

It's shown in the Appendix A.3,(156), that

$$T(l) = e^{-iPl/\hbar} \tag{124}$$

We can make condition the translation on the particle's spin by including in the exponent, the tensor product with P of an operator that leaves the particle's momentum as it already is if the particle is found in a spin-up state, and that changes the sign of the momentum operator if the particle is found in a spin-down state. This operator is

$$\sigma_z = |\uparrow\rangle\langle\uparrow| - |\downarrow\rangle\langle\downarrow| \tag{125}$$

which happens to be the Pauli spin matrix that corresponds to a measurement of the z-component of a spin-$\frac{1}{2}$ particle's spin. This gives us a conditional translation operator

$$S = e^{-i\sigma_z \otimes Pl/\hbar} \tag{126}$$

The direction of translation for this operator is now dependent on the particle's spin. It is shown in the appendix A.4 that we can rewrite this as

$$S = \left(|\uparrow\rangle\langle\uparrow| \otimes e^{-iPl}\right)\left(|\downarrow\rangle\langle\downarrow| \otimes e^{iPl}\right) \tag{127}$$

which shows that the action of S on the basis particle's basis states is defined by

$$|\uparrow\ \ x\rangle \to |\uparrow\ \ (x+l)\rangle \tag{128a}$$
$$|\downarrow\ \ x\rangle \to |\downarrow\ \ (m-1)\rangle \tag{128b}$$

Now consider an operator $R(\theta)$ that performs a rotation by an angle 2θ about the y-axis on the Bloch sphere

$$R(\theta) = \begin{pmatrix} \cos\theta & -\sin\theta \\ \sin\theta & \cos\theta \end{pmatrix} \tag{129}$$

If we assume that the particle is localized around x_0, and that we are going to rotate the apparatus that contains the particle, about the particle's y-axis by an angle 2θ, just after making a conditional translation on the particle's position, we have

$$\begin{aligned} R(\theta)\, S\, |\Psi\rangle &= \begin{pmatrix} \cos\theta & -\sin\theta \\ \sin\theta & \cos\theta \end{pmatrix} \left(|\uparrow\rangle \otimes a_\uparrow e^{-iPl} - |\downarrow\rangle \otimes a_\downarrow e^{iPl}\right) \otimes |x_0\rangle \\ &= \left[|\uparrow\rangle \otimes \left(a_\uparrow \cos\theta e^{-iPl} - a_\downarrow \sin\theta e^{iPl}\right) + |\downarrow\rangle \otimes \left(a_\uparrow \sin\theta e^{-iPl} + a_\downarrow \cos\theta e^{iPl}\right)\right] \otimes |x_0\rangle \end{aligned} \tag{130}$$

If we assume that the width of the wave packet is much bigger than the spatial translation l, then we can approximate $e^{\mp iPl} \approx I \mp iPl$. Using this assumption, we can rewrite (130) as

$$\begin{aligned} R(\theta)\, S\, |\Psi\rangle \approx\ & |\uparrow\rangle \otimes \left[\left(a_\uparrow \cos\theta - a_\downarrow \sin\theta\right) I - \left(a_\uparrow \cos\theta + a_\downarrow \sin\theta\right) iPl\right] \otimes |x_0\rangle \\ & + |\downarrow\rangle \otimes \left[\left(a_\uparrow \sin\theta + a_\downarrow \cos\theta\right) I - \left(a_\uparrow \sin\theta - a_\downarrow \cos\theta\right) iPl\right] \otimes |x_0\rangle \\ =\ & \left(a_\uparrow \cos\theta - a_\downarrow \sin\theta\right)\left[|\uparrow\rangle \otimes \left(I - iP\left[\frac{a_\uparrow \cos\theta + a_\downarrow \sin\theta}{a_\uparrow \cos\theta - a_\downarrow \sin\theta} l\right]\right)\right] \otimes |x_0\rangle \\ & + \left(a_\uparrow \sin\theta + a_\downarrow \cos\theta\right)\left[|\downarrow\rangle \otimes \left(I + iP\left[\frac{a_\downarrow \cos\theta - a_\uparrow \sin\theta}{a_\uparrow \sin\theta + a_\downarrow \cos\theta} l\right]\right)\right] \otimes |x_0\rangle \end{aligned} \tag{131}$$

This can be simplified by defining amplitudes

$$A_\uparrow = \left(a_\uparrow \cos\theta - a_\downarrow \sin\theta\right) \tag{132a}$$
$$A_\downarrow = \left(a_\uparrow \sin\theta + a_\downarrow \cos\theta\right) \tag{132b}$$

and length of translation

$$l_{\uparrow} = \frac{a_{\uparrow}\cos\theta + a_{\downarrow}\sin\theta}{a_{\uparrow}\cos\theta - a_{\downarrow}\sin\theta} l \tag{133a}$$

$$l_{\downarrow} = \frac{a_{\downarrow}\cos\theta - a_{\uparrow}\sin\theta}{a_{\uparrow}\sin\theta + a_{\downarrow}\cos\theta} l \tag{133b}$$

to represent the possible translations that can be observed after the system has been rotated relative to the measurement axis.

Using (133), the translation operators can now be re-expressed as

$$\begin{aligned} I - iPl_{\uparrow} &\approx e^{-iPl_{\uparrow}} \\ &= T\left(l_{\uparrow}\right) \end{aligned} \tag{134a}$$

$$\begin{aligned} I + iPl_{\downarrow} &\approx e^{iPl_{\downarrow}} \\ &= T\left(-l_{\downarrow}\right) \end{aligned} \tag{134b}$$

So that

$$\begin{aligned} R\left(\theta\right)U\left|\Psi\right\rangle &\approx A_{\uparrow}\left|\uparrow\right\rangle \otimes T\left(l_{\uparrow}\right)\left|x_0\right\rangle + A_{\downarrow}\left|\downarrow\right\rangle \otimes T\left(l_{\downarrow}\right)\left|x_0\right\rangle \\ &= A_{\uparrow}\left|\uparrow\right\rangle \otimes \left|x_0 + l_{\uparrow}\right\rangle + A_{\downarrow}\left|\downarrow\right\rangle \otimes \left|x_0 - l_{\downarrow}\right\rangle \end{aligned} \tag{135}$$

A measurement on the particle's spin gives

$$M_z R\left(\theta\right)U\left|\Psi\right\rangle = \begin{cases} \left|\uparrow\right\rangle \otimes \left|x_0 + l_{\uparrow}\right\rangle, & \text{with probability } \left|\left(a_{\uparrow}\cos\theta - a_{\downarrow}\sin\theta\right)\right|^2 \\ \left|\downarrow\right\rangle \otimes \left|x_0 - l_{\downarrow}\right\rangle, & \text{with probability } \left|\left(a_{\uparrow}\sin\theta + a_{\downarrow}\cos\theta\right)\right|^2 \end{cases} \tag{136}$$

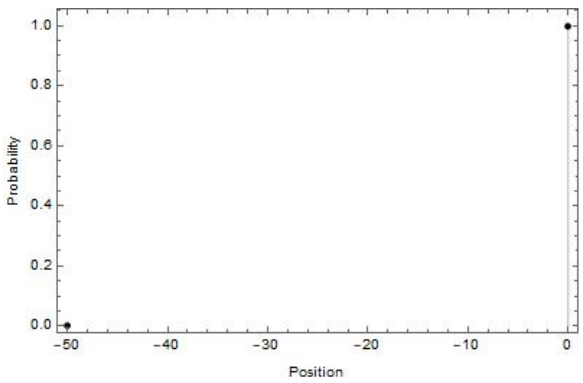

Figure 17: This figure shows the possible measurement outcomes predicted by (133). The parameters used here are $\theta = \frac{\pi}{4}$, $a_{\uparrow} = \sqrt{0.48}$ $a_{\downarrow} = \sqrt{0.52}$. According to this prediction, the particle will be found at $l_{\uparrow} = -49.98$ with probability 0.0004, and at $l_{\downarrow} = -0.02$ with probability 0.9996 .

The main idea is that right after the spatial translation, if we rotate the particle's spin basis relative to our measurement basis, before making the measurement, then it is possible to measure a translation that is much greater than the distance l. This quantum phenomenon is shown in Figure 17, which shows that there is a 0.04% probability that the translation will be about 50 times as large as it was intended to be if we rotate the system according to (129) before making the measurement.

2.10 Deriving the Klein-Gordon Equation from a Discrete-Time Quantum Walk on a Line

Multiple derivations of the Schrödinger, Klein-Gordon, and Dirac equations have been done starting from a discrete-time quantum walk on a line, among them [3, 15–17]. These derivations generally involve choosing a specific coin operator, setting up a difference quotient using the recursion relations predicted by the action of the coin operator on the wavefunction, and then taking the continuous limit to get a differential equation.

In this section we'll derive the Klein-Gordon equation starting from a discrete-time quantum walk defined by

$$\begin{pmatrix} \Psi^L_{m,j+1} \\ \Psi^R_{m,j+1} \end{pmatrix} = C(\theta) \begin{pmatrix} \Psi^L_{m+1,j} \\ \Psi^R_{m-1,j} \end{pmatrix} \tag{137}$$

where the coin operator $C(\theta)$ is defined as

$$C(\theta) = \begin{pmatrix} \cos\theta & -i\sin\theta \\ -i\sin\theta & \cos\theta \end{pmatrix} \tag{138}$$

Once expanded, (137) gives us two recursion relations

$$\Psi^L_{m,j+1} = \cos\theta \Psi^L_{m+1,j} - i\sin\theta \Psi^R_{m-1,j} \tag{139a}$$
$$\Psi^R_{m,j+1} = -i\sin\theta \Psi^L_{m+1,j} + \cos\theta \Psi^R_{m-1,j} \tag{139b}$$

These equations are similar to the recursion relation (25) that we set up to solve for the continuous limit of a classical random walk in Section 1.4. However, this time we have two equations instead of one, and they are coupled. Before setting up difference quotients we need to first decouple the two equations.

With this idea in mind, (139a), (139b) rearrange to

$$\Psi^R_{m-1,j} = \frac{i}{\sin\theta}\left(\Psi^L_{m,j+1} - \cos\theta \Psi^L_{m+1,j}\right) \tag{140a}$$
$$\Psi^L_{m+1,j} = \frac{i}{\sin\theta}\left(\Psi^R_{m,j+1} - \cos\theta \Psi^R_{m-1,j}\right) \tag{140b}$$

We can use (140a) to replace $\Psi^R_{m-1,j}$ on the right hand side of (139b), and (140b) to replace $\Psi^L_{m+1,j}$ on the right hand side of (139a). This leaves us still needing to replace $\Psi^L_{m,j+1}$ on the left hand side of (139a) and $\Psi^R_{m,j+1}$ on the left hand side of (139b).

We can get an equation for $\Psi^L_{m,j+1}$ by translating (140b) one unit backward along the space axis $m \to m-1$ and one unit forward along the time axis $j \to j+1$, which gives us (141b). Similarly, we can get an equation for $\Psi^R_{m,j+1}$ by translating (140a) one unit forward along both the time and space axes $m \to m+1, j \to j+1$, to get (141a).

$$\Psi^R_{m,j+1} = \frac{i}{\sin\theta}\left(\Psi^L_{m+1,j+2} - \cos\theta\Psi^L_{m+2,j+1}\right) \tag{141a}$$

$$\Psi^L_{m,j+1} = \frac{i}{\sin\theta}\left(\Psi^R_{m-1,j+2} - \cos\theta\Psi^R_{m-2,j+1}\right) \tag{141b}$$

Substituting (141a) and (141b) into the left hand side of (139b) and (139a), respectively, and then rearranging things gives

$$\Psi^R_{m-1,j+2} + \Psi^R_{m-1,j} - \cos\theta\left(\Psi^R_{m,j+1} + \Psi^R_{m-2,j+1}\right) = 0 \tag{142a}$$

$$\Psi^L_{m+1,j+2} + \Psi^L_{m+1,j} - \cos\theta\left(\Psi^L_{m+2,j+1} + \Psi^L_{m,j+1}\right) = 0 \tag{142b}$$

$$\Psi^R_{m-1,j+2} + \Psi^R_{m-1,j} - \cos\theta\left(\Psi^R_{m,j+1} + \Psi^R_{m-2,j+1}\right) = 0 \tag{143a}$$

$$\Psi^L_{m+1,j+2} + \Psi^L_{m+1,j} - \cos\theta\left(\Psi^L_{m+2,j+1} + \Psi^L_{m,j+1}\right) = 0 \tag{143b}$$

Adding

$$2\left(\Psi^R_{m-1,j+1} - \Psi^R_{m-1,j+1}\right) + 2\cos\theta\left(\Psi^R_{m-1,j+1} - \Psi^R_{m-1,j+1}\right) = 0 \tag{144a}$$

$$2\left(\Psi^L_{m+1,j+1} - \Psi^L_{m+1,j+1}\right) + 2\cos\theta\left(\Psi^L_{m+1,j+1} - \Psi^L_{m+1,j+1}\right) = 0 \tag{144b}$$

to the left hand sides of (142a),(142b) respectively, and then dividing both expressions by h^2 on either side, allows us to set up a difference quotient for each equation

$$\begin{aligned} 0 = {} & \frac{1}{h}\left(\frac{\psi^R_{m-1,j+2} - \psi^R_{m-1,j+1}}{h} - \frac{\psi^R_{m-1,j+1} - \psi^R_{m-1,j}}{h}\right) \\ & - \cos\theta\left[\frac{1}{h}\left(\frac{\psi^R_{m,j+1} - \psi^R_{m-1,j+1}}{h} - \frac{\psi^R_{m-1,j+1} - \psi^R_{m-2,j+1}}{h}\right)\right] \\ & + 2\left(1 - \cos\theta\right)\psi^R_{m-1,j+1} \end{aligned} \tag{145a}$$

and

$$\begin{aligned} 0 = {} & \frac{1}{h}\left(\frac{\psi^L_{m+1,j+2} - \psi^L_{m+1,j+1}}{h} - \frac{\psi^L_{m+1,j+1} - \psi^L_{m+1,j}}{h}\right) \\ & - \cos\theta\left[\frac{1}{h}\left(\frac{\psi^L_{m+2,j+1} - \psi^L_{m+1,j+1}}{h} - \frac{\psi^L_{m+1,j+1} - \psi^L_{m,j+1}}{h}\right)\right] \\ & + 2\left(1 - \cos\theta\right)\psi^L_{m+1,j+1} \end{aligned} \tag{145b}$$

We can now impose the condition $\Delta m = \Delta j = h$, and rewrite (145) as

$$\begin{aligned} 0 = &\frac{1}{\Delta j}\left(\frac{\psi m-1, j+2^R - \psi^R_{m-1,j+1}}{\Delta j} - \frac{\psi^R_{m-1,j+1} - \psi^R_{m-1,j}}{\Delta j}\right) \\ &- \cos\theta\left[\frac{1}{\Delta m}\left(\frac{\psi^R_{m,j+1} - \psi^R_{m-1,j+1}}{\Delta m} - \frac{\psi^R_{m-1,j+1} - \psi^R_{m-2,j+1}}{\Delta m}\right)\right] \\ &+ 2\left(1-\cos\theta\right)\psi^R_{m-1,j+1} \end{aligned} \tag{146a}$$

and

$$\begin{aligned} 0 = &\frac{1}{\Delta j}\left(\frac{\psi^L_{m+1,j+2} - \psi^L_{m+1,j+1}}{\Delta j} - \frac{\psi^L_{m+1,j+1} - \psi^L_{m+1,j}}{\Delta j}\right) \\ &- \cos\theta\left[\frac{1}{\Delta m}\left(\frac{\psi^L_{m+2,j+1} - \psi^L_{m+1,j+1}}{\Delta m} - \frac{\psi^L_{m+1,j+1} - \psi^L_{m,j+1}}{\Delta m}\right)\right] \\ &+ 2\left(1-\cos\theta\right)\psi^L_{m+1,j+1} \end{aligned} \tag{146b}$$

And now we can take the limit $\Delta j, \Delta m \to 0$ under the condition $\frac{\Delta m}{\Delta j} = 1$ (which is required by $\Delta m = \Delta j = h$). Doing this and then dividing both sides of the two equations by $\cos\theta$ puts them in the form

$$\frac{1}{\cos\theta}\frac{\partial^2\psi^R}{\partial t^2} - \frac{\partial^2\psi^R}{\partial x^2} + 2\frac{1-\cos\theta}{\cos\theta}\psi^R = 0 \tag{147a}$$

$$\frac{1}{\cos\theta}\frac{\partial^2\psi^L}{\partial t^2} - \frac{\partial^2\psi^L}{\partial x^2} + 2\frac{1-\cos\theta}{\cos\theta}\psi^L = 0 \tag{147b}$$

The two equations have the same form, which means we can further simplify things by defining

$$\boldsymbol{\psi} = \begin{pmatrix}\psi^L \\ \psi^R\end{pmatrix} \tag{148}$$

Setting $c^2 = \cos\theta$ and $\left(\frac{mc}{\hbar}\right)^2 = 2\frac{1-\cos\theta}{\cos\theta}$, (147) can be re-expressed as

$$\frac{1}{c^2}\frac{\partial^2\boldsymbol{\psi}}{\partial t^2} - \frac{\partial^2\boldsymbol{\psi}}{\partial x^2} + \left(\frac{mc}{\hbar}\right)^2\boldsymbol{\psi} = 0 \tag{149}$$

which is the Klein-Gordon equation.

References

[1] J. Kempe. "Quantum random walks: an introductory overview," Contemporary Physics **44**. 307-327. 2003.

[2] A. Romanelli, A.C. Sicardi Schifino, R. Siri, G. Abal, A. Auyuanet, R. Donangelo. "Quantum random walk on the line as a Markovian process." Physica A: Statistical Mechanics and its Applications, **338**, 3, p. 395-405.

[3] C.M. Chandrashekar. "Discrete-Time Quantum Walk - Dynamics and Applications." ArXiv e-prints, quant-ph/1001.5326. Jan 2010.

[4] A. Childs, E. Farhi, and S. Gutmann. "An example of the difference between quantum and classical random walks." Quantum Information Processing, 1:35, 2002. lanl-reportquant-ph/0103020.

[5] S. Ross. "A First Course in Probability." Boston: Pearson. 2014.

[6] P.C. Bressloff. "Diffusion in Cells: Random Walks and Brownian Motion." Jul 2014. Springer Science.

[7] E.W. Weisstein. "Random Walk–1-Dimensional." 2016. Retrieved from MathWorld–A Wolfram Web Resource: http://mathworld.wolfram.com/RandomWalk1-Dimensional.html

[8] S. Redner. Chapter 2: Random Walk/Diffusion. Fundamental kinetic processes. 2015. Retrieved from http://physics.bu.edu/ redner/542/book/rw.pdf

[9] C.P. Dettmann. "1D PDEs on infinite Domains: Fourier Transformations." Retrieved 2016, from University of Bristol: http://www.maths.bris.ac.uk/ macpd/apde2/chap4.pdf

[10] G. Di Molfetta., M. Brachet, F. Debbasch. "Quantum walks in artificial electric and gravitational fields". Physica A Statistical Mechanics and its Applications, 397:157-168, 2014.

[11] A. Ambainis, E. Bach, A. Nayak, A. Vishwanath, and J. Watrous. " One-dimensional quantum walks." In Proc.33th STOC, July 6-8, 2001, Hersonissos, Crete, Greece. Retrieved from: http://www.math.uwaterloo.ca/ anayak/papers/AmbainisBNVW01.pdf

[12] A. Nayak, and A. Vishwanath. "Quantum Walk on the Line." ArXiv e-prints:quant-ph/0010117. Oct 2000.

[13] T. D. Mackay. S. Bartlett, L. Stephenson. "Quantum walks in higher dimensions." Journal of Physics A Mathematical General, 35:2745-2753. Mar 2002.

[14] Y. Aharonov, L. Davidovich, and N. Zagury. "Quantum random walks." Phys. Rev. A, 48(2):16871690, 1993.

[15] C. M. Chandrashekar, S. Banerjee, and R. Srikanth. "Relationship between quantum walks and relativistic quantum mechanics," Phys. Rev. D **85** 5042-5045 (2010).

[16] U.V. Vazirani. Dirac Equation. 2007. Retrieved from Berkley EECS: http://people.eecs.berkeley.edu/ vazirani/f04quantum/notes/dirac.pdf

[17] G. di Molfetta, F. Debbasch. "Discrete-time quantum walks: Continuous limit and symmetries." Journal of Mathematical Physics. **53**, 12. December 2012.

A Derivations

A.1 Expectation value of a classical binomial distribution- approach 2

A less rigorous approach for computing $\langle x \rangle$, uses the fact that the laws of physics are invariant under spatial translation. Invariance under spatial translation means that computing $\langle x \rangle$ is equivalent to first finding $\langle x + N \rangle$, and then shifting the center of the probability distribution back to $x = 0$ by subtracting N from both sides. Substituting (4) into (5)

$$\begin{aligned} \langle x + N \rangle &= \sum_{i=0}^{2N} i \cdot Prob\left(x + N = i\right) \\ &= \sum_{i=0}^{2N} i \cdot \binom{N}{i} {p_r}^i \left(1 - p_r\right)^{N-i} \end{aligned} \tag{150}$$

which is the equation for a binomial distribution with parameters $2N, p_r$, and means that $\langle x + N \rangle = 2Np_r$.[5] And linearity of the expectation value means that $\langle x + N \rangle = \langle x \rangle + \langle N \rangle$. Therefore

$$\begin{aligned} \langle x \rangle &= \langle x \rangle + \langle N \rangle - \langle N \rangle \\ &= \langle x + N \rangle - \langle N \rangle \\ &= 2Np_r - N \\ &= N\left[p_r - \left(1 - p_r\right)\right] \\ &= N\left(p_r - p_l\right) \end{aligned} \tag{151}$$

A.2 Using the binomial distribution's moment generating function to calculate $\left\langle {n_r}^2 \right\rangle$

The moment generating function for the distribution of a binomial random variable x with parameters (N, p) is given by $\langle x \rangle = Np \left\langle (y+1)^{i-1} \right\rangle$, where y is a binomial random variable with parameters $(N-1, p)$.

$$\begin{aligned} \left\langle {n_r}^2 \right\rangle &= Np_r \left\langle {n_r}' + 1 \right\rangle \\ &= Np_r \left(\left\langle {n_r}' \right\rangle + 1 \right) \end{aligned} \tag{152}$$

where ${n_r}'$ is a binomial random variable with parameters $(N-1, p_r)$, so $\left\langle {n_r}' \right\rangle = \left(N-1\right) p_r$. Substituting this into (152) gives

[5] The expectation value for a binomial random variable $X \sim B\left(n, p\right)$ is $\langle X \rangle = np$.

$$\left\langle {n_r}^2 \right\rangle = N p_r \left[(N-1) p_r + 1 \right] \tag{153}$$

which is the same result as (14).

A.3 Proof that $T(l) = e^{-\frac{iPl}{\hbar}}$

Lemma 1: $T^\dagger(l) = T(-l)$

Proof:

Using the fact that position state wavefunctions expressed in the position basis are delta functions

$$\begin{aligned} \langle y|T(-l)|x\rangle &= \langle y|x-l\rangle \\ &= \delta\left((x-l)-y\right) \\ &= \delta\left(x-(y+l)\right) \\ &= \langle y+l|x\rangle \\ &= \left(T(l)\,|y\rangle\right)^\dagger |x\rangle \\ &= \langle y|T^\dagger(l)|x\rangle \end{aligned} \tag{154}$$

The first and last matrix elements in (154) are equal, so $T^\dagger(l) = T(-l)$.

Lemma 2: $T(l)$ is unitary.

Proof:

Using Lemma 1

$$\begin{aligned} T(l)T^\dagger(l)\,|x\rangle &= T(l)T(-l)\,|x\rangle \\ &= T(l)\,|k-l\rangle \\ &= |x\rangle \\ &= I\,|x\rangle \end{aligned} \tag{155}$$

$T(l)\,T^\dagger(l) = I$ means that $T^\dagger(l) = T^{-1}(l)$ and so $T(l)$ is unitary.

The fact that $T(l)$ is unitary means that it has an exponential form

$$T(l) = e^{-iPl/\hbar} \tag{156}$$

for some Hermitian operator $-Pl/\hbar$. As it turns out, P is the momentum operator, which can be shown by showing that the position space eigenfunctions of P are the same plane waves as the eigenstates of the momentum operator. From (156), this makes momentum the infinitesimal generator of spatial translations.

A.4 Proof that $e^{-i(|\uparrow\rangle\langle\uparrow|-|\downarrow\rangle\langle\downarrow|)\otimes Pl} = \left(|\uparrow\rangle\langle\uparrow| \otimes e^{-iPl}\right) \cdot \left(|\downarrow\rangle\langle\downarrow| \otimes e^{+iPl}\right)$

Starting from (157)

$$S = e^{-i\sigma_z \otimes Pl/\hbar} \tag{157}$$

and using $\sigma_z = (|\uparrow\rangle\langle\uparrow| - |\downarrow\rangle\langle\downarrow|)$, we have

$$S = e^{-i(|\uparrow\rangle\langle\uparrow|-|\downarrow\rangle\langle\downarrow|)\otimes Pl} \tag{158}$$

If A, B commute, then $e^{A+B} = e^A + e^B$ [1]. Using this identity we can write

$$\begin{aligned} S &= e^{-i|\uparrow\rangle\langle\uparrow|\otimes Pl} e^{+i|\downarrow\rangle\langle\downarrow|\otimes Pl} \\ &= \left(\sum_{n=0}^{\infty} \frac{(-i\,|\uparrow\rangle\langle\uparrow| \otimes Pl)^n}{n!}\right) \cdot \left(\sum_{m=0}^{\infty} \frac{(i\,|\downarrow\rangle\langle\downarrow| \otimes Pl)^m}{m!}\right) \\ &= \left(\sum_{n=0}^{\infty} \frac{|\uparrow\rangle\langle\uparrow| \otimes (-iPl)^n}{n!}\right) \cdot \left(\sum_{m=0}^{\infty} \frac{|\downarrow\rangle\langle\downarrow| \otimes (iPl)^m}{m!}\right) \end{aligned} \tag{159}$$

where the last step is a result of $(|\uparrow\rangle\langle\uparrow|)^n = |\uparrow\rangle\langle\uparrow|$ and $(|\downarrow\rangle\langle\downarrow|)^m = |\downarrow\rangle\langle\downarrow|$, which follows from the fact that $|\uparrow\rangle\langle\uparrow|$ and $|\downarrow\rangle\langle\downarrow|$ are projectors, which by definition satisfy the condition $P^2 = P$. Pulling the dyads out of the summations, we have

$$\begin{aligned} S &= \left(|\uparrow\rangle\langle\uparrow| \otimes \sum_{n=0}^{\infty} \frac{(-iPl)^n}{n!}\right) \cdot \left(|\downarrow\rangle\langle\downarrow| \otimes \sum_{m=0}^{\infty} \frac{(iPl)^m}{m!}\right) \\ &= \left(|\uparrow\rangle\langle\uparrow| \otimes e^{-iPl}\right) \cdot \left(|\downarrow\rangle\langle\downarrow| \otimes e^{+iPl}\right) \end{aligned} \tag{160}$$